

1001513



This is to certify that the  
thesis entitled  
Spectrophotometric, Electrochemical, Photoelectrochemical,  
and Surface Analysis Studies of Copper  
Phthalocyanine/Metal Oxide Electrodes

presented by

Vance Roger Shepard, Jr.

has been accepted towards fulfillment  
of the requirements for

M.S. degree in Chemistry

A handwritten signature in black ink, appearing to read "Vance R. Shepard, Jr.", written over a horizontal line.

Major professor

Date 11/1/77

SPECTROPHOTOMETRIC, ELECTROCHEMICAL, PHOTOELECTROCHEMICAL,  
AND SURFACE ANALYSIS STUDIES OF COPPER  
PHTHALOCYANINE/METAL OXIDE ELECTRODES

By  
Vance Rogers Shepard, Jr.

A THESIS

Submitted to  
Michigan State University  
in partial fulfillment of the requirements  
for the degree of

MASTER OF SCIENCE

Department of Chemistry

1977

## ABSTRACT

### SPECTROPHOTOMETRIC, ELECTROCHEMICAL, PHOTOELECTROCHEMICAL, AND SURFACE ANALYSIS STUDIES OF COPPER PHTHALOCYANINE/METAL OXIDE ELECTRODES

By

Vance Rogers Shepard, Jr.

There has been a growing interest in the study of chemically-modified electrode surfaces. Irreversible adsorption or covalent-attachment of various molecules to an electrode surface can impart specific catalytic properties which the electrode alone did not possess. Copper phthalocyanine (CuPc) in its solution form, strongly adsorbed, or covalently-attached to a metal oxide electrode ( $\text{SnO}_2$  or  $\text{TiO}_2$ ) was studied. Spectrophotometric methods aided in determination of the number of adsorbed or covalently-attached dye molecules present on the electrode surface. Differential capacitance measurements for  $\text{SnO}_2$  and  $\text{TiO}_2$  and cyclic voltammetry of the tetrasodium salt of tetrasulfonated copper phthalocyanine ( $\text{CuPc}(\text{SO}_3^- \text{Na}^+)_4$ ) in DMSO and  $\text{H}_2\text{O}$  resulted in energy mapping of the semiconductor band structure in relation to the redox couples of the dye. Cyclic voltammetry of adsorbed and covalently-attached dye indicated retention of an electrochemically active species on the surface. ESCA analysis of electrodes in various states of electrochemical treatment showed two types of phthalocyanine present and variation in the copper valence

state with change of solvent. Photocurrents were generated by the adsorbed and covalently-attached CuPc electrodes. Photocurrent studies indicated a potential dependent decomposition/desorption process of the adsorbed dye electrodes. A steady potential dependent response was observed for the covalently-attached CuPc electrodes.

Dedication  
To Mom and Dad

## "ACKNOWLEDGMENTS"

I would like to thank Neil and Monty for their advice and encouragement. I would like to thank my parents, grandparents, Mrs. Elmer Clark, Mr. Alden Eddy and friends for their encouragement, faith, and thoughts. And many thanks to Victoria for her help in the preparation of this thesis.

## "TABLE OF CONTENTS"

	Page
CHAPTER I. INTRODUCTION. . . . .	1
A. Semiconductors (n-Type). . . . .	2
B. Chemical Modification of Electrode Surfaces. . . . .	5
C. ESCA . . . . .	7
D. Photocurrent Response Studies. . . . .	8
E. Phthalocyanines. . . . .	10
CHAPTER II. EXPERIMENTAL . . . . .	16
A. Dyes . . . . .	17
B. Solvents and Electrolytes. . . . .	18
C. Spectrophotometric Studies . . . . .	18
D. Electrochemical Studies. . . . .	19
E. Covalent-Attachment. . . . .	20
1. Sulfonamide Attachment . . . . .	21
2. Thiol. . . . .	21
F. Photocurrent Studies . . . . .	22
G. ESCA Analysis. . . . .	22
CHAPTER III. RESULTS AND DISCUSSION. . . . .	25
A. Solution Studies . . . . .	26
1. Spectrophotometric Studies of $\text{CuPc}(\text{SO}_3^- \text{Na}^+)_4$ . . . . .	26
2. Electrochemistry of $\text{CuPc}(\text{SO}_3^- \text{Na}^+)_4$ . . . . .	26

B.	Adsorbed Dye Studies. . . . .	41
1.	Spectrophotometric Studies of CuPc(SO <sub>3</sub> <sup>-</sup> Na <sup>+</sup> ) <sub>4</sub> . . . . .	41
2.	Electrochemistry of CuPc on SnO <sub>2</sub> . . . . .	43
3.	ESCA of CuPc on SnO <sub>2</sub> . . . . .	45
4.	Photocurrent Response of CuPc on SnO <sub>2</sub> . . . . .	52
C.	Covalent-Attachment Studies . . . . .	58
1.	Spectrophotometric Studies of Covalently-Attached CuPc. . . . .	58
2.	Electrochemistry of Covalently- Attached CuPc-SnO <sub>2</sub> Electrodes . . . . .	60
3.	Photocurrent Response . . . . .	64
CHAPTER IV. SUGGESTIONS FOR FUTURE WORK . . . . .		67
LIST OF REFERENCES. . . . .		69

"LIST OF TABLES"

	Page
Table 1. ESCA Data CuPc/SnO <sub>2</sub> . . . . .	49

"LIST OF FIGURES"

	Page
Figure 1. Energy diagram of semiconductor-electrolyte interface. . . . .	4
Figure 2. Structure of phthalocyanine. . . . .	11
Figure 3. CuPc covalent-attachment schemes . . . . .	15
Figure 4. Absorption spectra of $\text{CuPc}(\text{SO}_3^- \text{Na}^+)_4$ in DMSO and $\text{H}_2\text{O}$ . . . . .	27
Figure 5. Cyclic voltammetry of $\text{CuPc}(\text{SO}_3^- \text{Na}^+)_4$ in $0.1 \mu\text{ TEAP/DMSO}$ at (a) $\text{SnO}_2$ , (b) $\text{TiO}_2$ , and (c) Pt . . . . .	30
Figure 6. Cyclic voltammetry of $\text{CuPc}(\text{SO}_3^- \text{Na}^+)_4$ in $\text{H}_2\text{O}$ (pH 4) at (a) $\text{SnO}_2$ and (b) $\text{TiO}_2$ . . . . .	32
Figure 7. Differential capacitance vs potential plots of $\text{SnO}_2$ in $0.1 \mu\text{ TEAP/DMSO}$ and $\text{H}_2\text{O}$ (pH 4) .	35
Figure 8. Differential capacitance vs potential plots of $\text{TiO}_2$ in $0.1 \mu\text{ TEAP/DMSO}$ and $\text{H}_2\text{O}$ (pH 4) .	37
Figure 9. Energy diagram of $\text{CuPc}(\text{SO}_3^- \text{Na}^+)_4$ redox couples in $0.1 \mu\text{ TEAP/DMSO}$ at $\text{SnO}_2$ , $\text{TiO}_2$ and Pt . .	39
Figure 10. Energy diagram of $\text{CuPc}(\text{SO}_3^- \text{Na}^+)_4$ oxidation in $\text{H}_2\text{O}$ (pH 4) at $\text{SnO}_2$ and $\text{TiO}_2$ . . . . .	40
Figure 11. Absorption spectra of clean $\text{SnO}_2$ and CuPc sublimed on $\text{SnO}_2$ electrodes . . . . .	42
Figure 12. Cyclic voltammetry of CuPc sublimed on $\text{SnO}_2$ in $0.1 \mu\text{ TEAP/DMSO}$ . . . . .	44
Figure 13. $\text{Cu}(2p_{1/2,3/2})$ ESCA spectra of. . . . .	48
Figure 14. $\text{N}(1s)$ ESCA spectra of. . . . .	51

Figure 15.	Photocurrent response of a CuPc/SnO <sub>2</sub> electrode in 0.05 Na <sub>2</sub> C <sub>2</sub> O <sub>4</sub> /pH 7 buffer. . . . .	53
Figure 16.	Photocurrent response vs anodic bias potential plots of two CuPc/SnO <sub>2</sub> electrodes in 0.05M Na <sub>2</sub> C <sub>2</sub> O <sub>4</sub> /pH 7 buffer. . . . .	56
Figure 17.	Absorption spectra of clean SnO <sub>2</sub> and covalently-attached-SnO <sub>2</sub> electrodes . . . . .	59
Figure 18.	Cyclic voltammetry of a covalently-attached CuPc-SnO <sub>2</sub> electrode in 0.1 μ TEAP/DMSO . . . . .	62
Figure 19.	Photocurrent response vs anodic bias potential of a covalently-attached CuPc-SnO <sub>2</sub> electrode. . . . .	66

CHAPTER I  
INTRODUCTION

The photodecomposition of water into its elements ( $H_2$ ,  $O_2$ ) is one of the most attractive means of storing solar energy. This decomposition process may be broken down into three steps: light absorption, water oxidation, and water reduction. Metal oxides ( $SnO_2$  and  $TiO_2$ ) doped as n-type semiconductors have catalyzed the decomposition of  $H_2O$  (1). Certain dyes, by virtue of their high absorption in the visible region and their facility in undergoing oxidation-reduction reactions, should also be capable of mediating some or all of these processes. Dye in solution (2), adsorbed (3), and covalently-attached (4, 5) at metal or semiconductor electrodes have been used to generate photocurrents. A brief discussion of semiconductor electrochemistry, covalent-attachment (chemical modification), and photocurrents is essential for a better understanding of light energy conversion. A useful tool for surface analysis, electron spectroscopy for chemical analysis (ESCA), is also discussed.

### Semiconductors(n-Type)

Great progress in semiconductor electrochemistry has been made since realization of their potential use in solar cells. Various n-type semiconductors such as  $SnO_2$  and  $TiO_2$  have been used extensively for studies in both aqueous and nonaqueous media (6). Electrode processes on semiconductors show certain characteristics that are different from those of electrode reactions on metals. The main

difference in reactions on metals and on semiconductors is that in the latter, the kinetics of the reaction may depend on processes that occur within the solid electrode.

A bending of the bands occurs at the surface of a semiconductor in contact with an electrolyte. Application of an anodic potential results in formation of a depletion or positive charged layer at the semiconductor surface (or in the space charge region within it), thus leading to upward bending of the bands (Figure 1). Application of a cathodic potential gives rise to a downward bending of the bands due to formation of a negative charge layer (7).

When a semiconductor is in contact with an electrolyte, a significant part of the potential drop is across the space charge region within the semiconductor; the rest is across the double layer on the electrolyte side. In experimental investigations of the double layer at semiconductor-electrolyte interfaces, an important parameter is the capacitance of the interface,  $C$ , which varies as a function of electrode potential  $V$ . The measured capacitance  $C$  is composed of  $C_{sc}$ , capacitance of space charges in the semiconductor, and  $C_H$ , the capacitance of the Helmholtz double layer on the solution side of the interface. Since the capacitances are in series and  $C_{sc}$  is usually small as compared to  $C_H$ , the measured capacitance ( $C$ ) is essentially equal to  $C_{sc}$  (7).

A differential capacitance plot of  $1/C_{sc}^2$  vs potential according to the Mott-Schottky equation

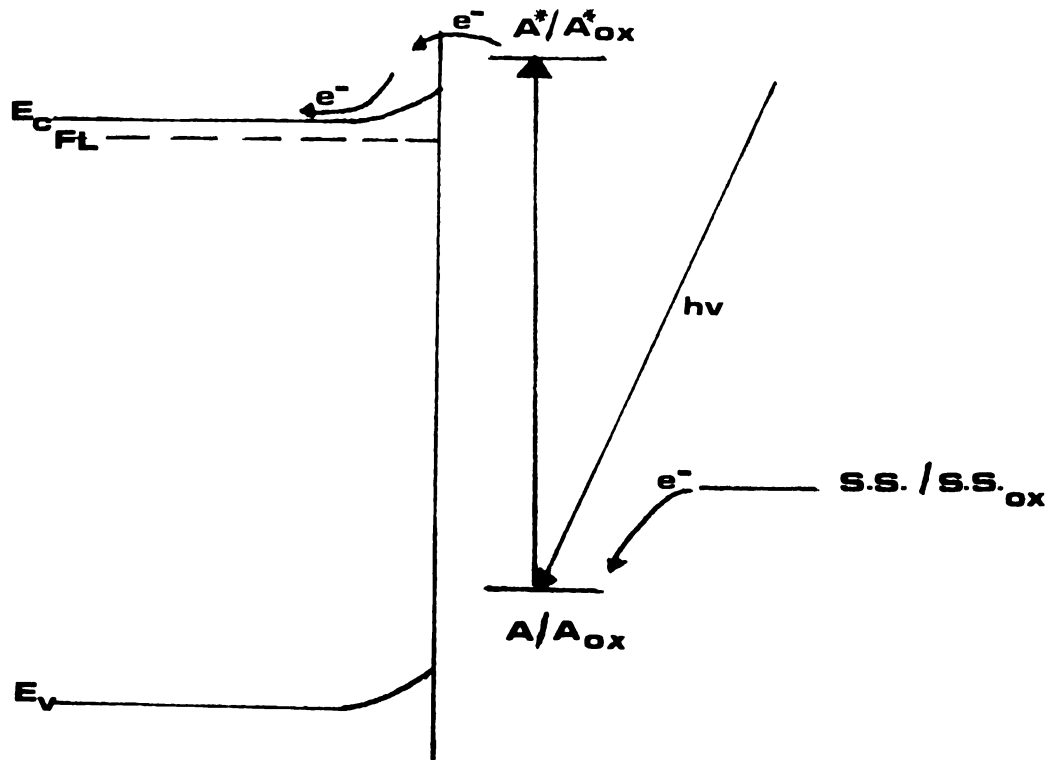


Figure 1. Energy diagram of semiconductor-electrolyte interface.

$$1/C_{sc}^2 = 2/\epsilon\epsilon_0 e_0 n_0 \phi_s - kT/e_0$$

yields information about the effective carrier density  $n_0$  from the slope of the plot and flatband potential  $V_{fb}$  from the potential axis intercept. The flatband potential is the potential at which excess electrical charge in the semiconductor is zero and is indicative of the position of the Fermi level in the semiconductor band gap region with respect to the reference electrode.  $C_{sc}$  is the capacitance of the semiconductor electrode,  $\epsilon$  and  $\epsilon_0$  are the dielectric constant of the semiconductor and permittivity of free space, respectively,  $e_0$  is the absolute value of the electronic charge,  $n_0$  is the donor density,  $k$  is the Boltzmann constant, and  $\phi_s$  is the potential difference between the flatband potential and the potential at which the measurement is made (7, 8).

### Chemical Modification of Electrode Surfaces

Chemical modification of surfaces is useful in research areas such as chromatography and catalysts. Chemically-modified solid supports have been used to improve chromatographic column performance. This has depended on an organosilane reaction with the surfaces of silica or alumina particles. Homogeneous catalysts have been attached to silica to provide heterogeneous hydroformylation catalysts (9). Acid-base dye indicators have been attached to silica surfaces to create solid indicators (10).

Electrochemistry is a field where chemically-modified

surfaces are of great value. Chemical modification of an electrode surface refers to strong binding of a selected chemical reagent to the surface to endow it with some or all of the chemical and electrochemical properties of the selected reagent. Such chemically-modified electrodes represent new approaches to the study of electrochemical reactions.

Modification based on covalent bond formation between the reagent and electrode has been described for carbon (11), SnO<sub>2</sub> (12,13), and TiO<sub>2</sub> (14). Optically active amino acids have been bound to carbon electrodes via amide bonds to form a chiral electrode (15). The work on SnO<sub>2</sub> and TiO<sub>2</sub> electrodes utilize organosilane reagents, which bear amine, pyridyl, mercapto, and other functional groups. Schematically the reaction of an organosilane with a surface hydroxyl group can be represented as



The modified surface chemical stability is quite good except in the presence of strong acid or base solution (13).

Rhodamine B and iron porphyrin have been attached to SnO<sub>2</sub> via an amide bond (4,16). Recently, Hawn and Armstrong attached erythrosin to SnO<sub>2</sub> using either an amide or a thiol linkage (5). These chemically-modified electrodes have displayed some very interesting electrochemical and photoelectrochemical results in which the electrodes appear to be chemically stable.

ESCA

The ESCA (electron spectroscopy for chemical analysis) technique was originated and developed by Siegbahn and co-workers in Sweden during the 1960's (17,18). In ESCA, nearly monochromatic x-radiation of 1254eV (Mg  $K\alpha_{1,2}$ ) energy impinge on a surface. Radiation in this range provides sufficient energy for the ejection of core electrons. Although the x-rays penetrate to thousands of angstroms, the photoelectrons produced have an escape mean free path of only 5  $\text{\AA}$  to 100  $\text{\AA}$ , depending on the material. Core electrons kinetic energies,  $E_k$ , are measured accurately, making it possible to determine the binding energies,  $E_b$ , of the core electrons from the relation

$$E_b = h\nu - E_k - \phi_{sp}$$

where  $\phi_{sp}$  is the work function or energy necessary to raise a free electron from the Fermi level to vacuum level .

Binding energies are responsive to changes in the chemical environment. Shifts in binding energies are produced by the charge and valence state of an atom and the electronic relaxation effect from neighboring atoms. This refers to the effect of electronic charge flow from neighboring atoms to the core hole in the positive ion produced by the photo-emission (19,20).

ESCA is sensitive to all the elements but hydrogen and helium. Since the measured electron binding energies of most elements are unique, a broad range scan of electron energy spectrum provides a good means of qualitative

analysis. The sensitivity of ESCA is on the order of  $10^{-6}$  grams. The integrated intensities of the electron signals are directly proportional to the number of similar atoms in the sample, representing a pseudo-quantitative tool. To insure minimum surface contamination, mainly carbon, a  $10^{-8}$  to  $10^{-10}$  torr vacuum is required in the sample chamber. Samples may be cleaned or depth profiled by an argon sputter gun (19).

ESCA has been used extensively in adsorption (21), surface oxide (22), and catalysts (23) studies. Surfaces of clean (12,24) and chemically-modified (13,11) semiconductor electrodes have been characterized. This has led to a better understanding of the chemical and physical structure of these surfaces.

### Photocurrent Response Studies

n-Type semiconductors such as  $\text{TiO}_2$  and  $\text{SnO}_2$  will catalyze the oxidation of water when irradiated with greater than bandgap light energy (1,25). The electrooxidation of water occurs as a result of vacancies produced in the valence band of the highly-doped semiconductor (7). A depletion or space charge layer is maintained at the electrode surface by means of an applied bias potential. Under these conditions, the conduction band remains charge depleted, and holes created in the valence band move to the surface and accept charge in the oxidation of  $\text{H}_2\text{O}$  or  $\text{OH}^-$ .

It is well known that certain photoexcited dye molecules in the vicinity of the electrode interface are capable of

transferring charge to the conduction band of an n-type semiconductor electrode (2, 26). Figure 1 explains this process in terms of an energy diagram with the redox reactions of the dye in both the ground and excited states. Photoexcitation of the dye occurs at light energies less than the semiconductor band gap energy. The excited dye is then capable of losing an electron to the conduction band of the semiconductor.

Anodic bias results in charge depletion of the conduction band, and electron flow is from the dye towards the semiconductor conduction band. Photocurrent response as a function of wavelength usually parallels the absorption spectrum of the dye (2). If a reducing agent such as sodium oxalate is present in solution with the dye, enhanced photocurrents are observed (supersensitization). This is due to a continual regeneration of the ground state of the dye by the reducing agent. The kinetics of the supersensitization reaction depend upon the extent of overlap of the energy distribution of the excited dye molecule population, redox states of the reducing agent, and appropriate energy level distribution of the semiconductor (26).

Photocurrent response studies have been carried out on dyes in solution (2, 26), adsorbed (3), or covalently-attached (4) at both metal and semiconductor electrodes. All of the dyes absorb strongly in the visible region. Large extinction coefficients are necessary for maximum capture of the sensitizing radiation. In most cases,

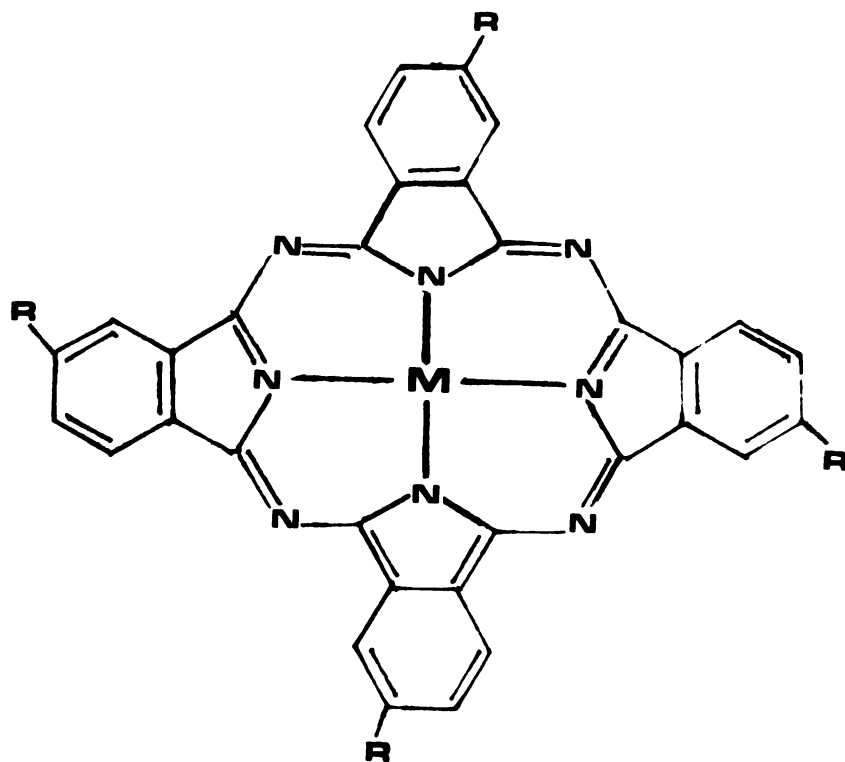
multilayers of dye result in increased quenching and an ohmic resistance for electron transfer is formed. This prevents fast removal of electronic charge from the dye layer (2).

### Phthalocyanines

Phthalocyanine is a large organic heterocycle containing  $\pi$  electrons. Transition metal and post-transition metal ions can be coordinated within this ring (Figure 2) (27); these highly colored compounds are unique in many ways. They are insoluble in most organic solvents and only slightly soluble in solvents such as o-dichlorobenzene and pyridine. Various functional groups such as halogens, amines, sulfonic and carboxylic acids can be substituted for hydrogens on the four benzene rings (Figure 2) (27). These functional groups greatly affect the color and solubility of the phthalocyanines. Colors vary from greens to blues; this is important in the dye industry where the phthalocyanines have their greatest use.

Absorption spectra of phthalocyanines in solution and sublimed on glass have been reported (28,29). They absorb strongly in the visible region, having large extinction coefficients ( $30,000\text{M}^{-1}\text{cm}^{-1}$  -  $150,000\text{M}^{-1}\text{cm}^{-1}$ ). The strongest absorption is in the 600nm-750nm (2.1ev-1.8ev) region and corresponds to  $\pi \rightarrow \pi^*$  transitions of the ring system (30).

Cyclic voltammetry studies of  $\text{CuPc}(\text{SO}_3^- \text{Na}^+)_4$  in .1 TEAP/DMSO at mercury show two reversible one-electron reductions



**R=** H, SO<sub>3</sub>H, I, SO<sub>2</sub>Cl, etc.

**M=** Cu<sup>+2</sup>, Co<sup>+2</sup>, Ge<sup>+4</sup>, Si<sup>+4</sup>, etc.

Figure 2. Structure of phthalocyanine.

and an oxidation (30). Chemical stability of the monoanion, dianion, and monocation is indicated by the reversible redox couples. The anodic redox couple of copper, zinc, and nickel phthalocyanine was inaccessible due to use of a mercury electrode. Absorption spectra of negative ions formed by sodium reduction of various phthalocyanines have indicated addition of electrons to the ring system and not the central atom (31).

The ability for electrochemical reduction of oxygen by organic semiconductors such as phthalocyanines has attracted the attention of many researchers in connection with their possible use in fuel cells (32,33,34). Much of the phthalocyanine electrochemistry reported is centered around this. Photoinduced reduction has been done on phthalocyanine films on carbon and platinum in various pH buffers. It has been shown that the catalytic properties of phthalocyanines are largely determined by the nature of the central atom (35). The order of decreasing electrocatalytic activity is  $\text{Fe} > \text{Co} > \text{Ni} > \text{Cu} > \text{H}_2(\text{metal-free})$ . This has indicated that phthalocyanines with higher magnetic moments (or paramagnetic susceptibility) appear to exhibit electrocatalytic activity toward the oxygen reduction reaction (36).

Recently, attachment of cobalt phthalocyanine to cross-linked polyacrylamide produced a stable oxidation catalyst with enhanced activity. It was coupled by means of cyanuric chloride to  $\text{NH}_2$  groups of the polymer matrix (37).

ESCA analysis of phthalocyanines sublimed on copper has

shown two types of nitrogen present in metal-free phthalocyanine (four equivalent central nitrogens and four equivalent meso-bridging nitrogens). Presence of a metal atom in the ring equalizes the energy of these nitrogens and results in a sharp nitrogen (1s) peak with a weak satellite (38, 39).

The choice of copper phthalocyanine for use in our studies was for the following reasons: 1) structural similarity to naturally-occurring porphyrins, 2) large extinction coefficient, 3) ease of copper detection in surface analysis by ESCA. Our initial investigations of the CuPc in its solution form, strongly adsorbed, or covalently-attached to  $\text{SnO}_2$  or  $\text{TiO}_2$  electrodes are discussed. Spectrophotometric studies were used to determine regions of maximum absorption and extinction coefficients for the CuPc solutions and electrodes. Absorbance values were used to determine the number of dye molecules present on the adsorbed or covalently-attached dye/ $\text{SnO}_2$  electrodes.

Differential capacitance plots for  $\text{SnO}_2$  and  $\text{TiO}_2$  gave information concerning the band structure: the Fermi level position and  $n_0$ , the donor density. Cyclic voltammetry of  $\text{CuPc}(\text{SO}_3^- \text{Na}^+)_4$  in DMSO and  $\text{H}_2\text{O}$  was done to determine the positions of the redox couples at  $\text{SnO}_2$ ,  $\text{TiO}_2$ , and Pt. From these, energy diagrams showing the relation between the semiconductor band structure and redox couples of the dye could be drawn.

CuPc sublimed on  $\text{SnO}_2$  was used in cyclic voltammetric

studies and the behavior compared to that of the solution form. ESCA analysis of electrodes in various states of electrochemical pretreatment in DMSO and H<sub>2</sub>O along with standards was done to aid in understanding their electrochemical behavior.

Covalent-attachment of CuPc to SnO<sub>2</sub> and TiO<sub>2</sub> was attempted via a sulfonamide or thiol formation using the sulfonyl chloride or tetraiodated form of the dye, respectively (Figure 3). The dye was coupled to the surface using various organosilanes which had either a terminal amine or mercapto functional group.

Cyclic voltammetry of the covalent-attached dye-semiconductor electrodes was carried out to determine the chemical stability and position of redox couples. The behavior of the covalently-attached dye was compared to that of the solution and adsorbed form.

The spectrophotometric, electrochemical, and ESCA studies characterized the behavior of the dye in its various forms. This facilitated understanding of the photocurrent response data. Photocurrents of adsorbed and covalently-attached CuPc-SnO<sub>2</sub> electrodes in pH 7 buffer as a function of anodic bias potential were explored. A reducing or supersensitizing agent such as sodium oxalate was added to enhance the photocurrent response.

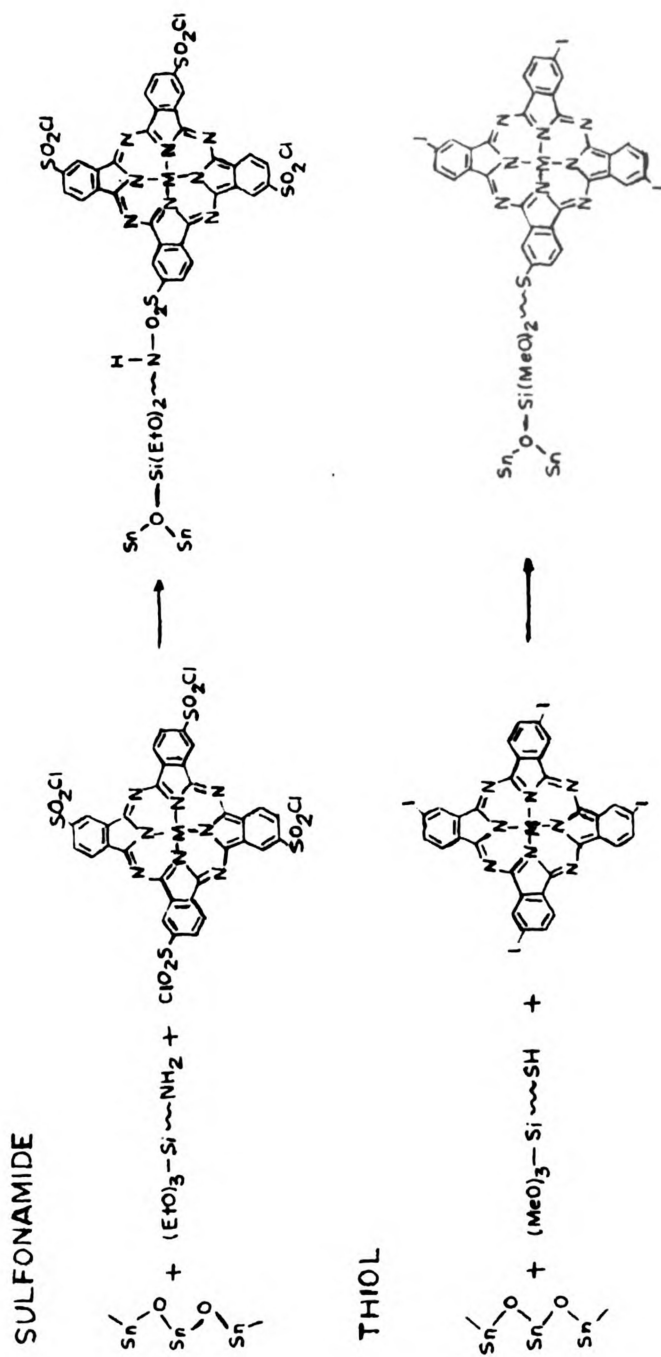


Figure 3. CuPc covalent-attachment schemes

CHAPTER II  
EXPERIMENTAL

Dyes

Copper phthalocyanine was obtained from Eastman Kodak. 4,4',4'',4'''-tetrasulfonated copper phthalocyanine ( $\text{CuPc}(\text{SO}_3^- \text{Na}^+)_4$ ) was synthesized according to the procedure of Weber and Busch (40). The monosodium salt of 4-sulfophthalic acid (0.162 mole), ammonium chloride (0.09 mole), urea (0.97 mole), ammonium molybdate (0.0006 mole), and copper sulfate 5-hydrate (0.048 mole) were added to 40 ml of nitrobenzene and heated at 180°C for six hours. The crude product was then washed with methanol, 1N hydrochloric acid, saturated with sodium chloride and then dissolved in 0.1N sodium hydroxide. After the solution was heated to 80°C and filtered, sodium chloride was added to precipitate the solid product. The pure blue product was filtered, washed with aqueous ethanol, and dried in vacuo overnight.

4-iodophthalic anhydride needed for the synthesis of tetra-4-iodo-copper phthalocyanine was prepared by the method of Higgins and Hilton (41). 5-iodo-anthranilic acid (0.12 mole) was added to 500 ml of 3.3M sulfuric acid and cooled to 5°C. After the addition of 23 g of sodium nitrite and stirring for two hours, the diazonium solution was poured onto crushed ice and raised to a pH of 6.5 with sodium hydroxide. A complex cyanide solution was added and the diazonium salt solution was heated, cooled, and acidified. The resulting solid product was added to a dry benzene and acetic anhydride solution, refluxed, and cooled to give 4-iodophthalic anhydride. Tetra-4-iodo-copper phthalocyanine was prepared by

the method of Suzuki and Bansho (42). 4-iodophthalic anhydride (13.2 g), urea (23 g), copper (II) chloride 2-hydrate (4 g), 1,2,4-trichlorobenzene (400 g), and titanium (IV) chloride (0.2 g) were heated to 160°C for one hour, kept at 177-188°C for fifty minutes, filtered, and washed with benzene, methanol, 3% hydrochloric acid, water, and ethanol. The solid blue-green product was dried in vacuo overnight.

### Solvents and Electrolytes

Spectrargrade dimethylsulfoxide (DMSO) was obtained from Burdick and Jackson Labs. It was purified by passing through an activated alumina column and then stored over activated 4 Å molecular sieves. The water used was distilled and passed through a Milli Pore Milli Q system containing an anion exchanger, cation exchanger, and activated charcoal. Reagent grade tetraethylammonium perchlorate (TEAP) was recrystallized from ethanol and dried at 80°C overnight. Reagent grade nitric acid, sodium hydroxide, sodium bicarbonate, potassium dihydrogen phosphate were used as was for the pH 4 and 7 buffer solutions.

### Spectrophotometric Studies

Spectra of  $\text{CuPc}(\text{SO}_3^- \text{Na}^+)_4$  and  $\text{CuPcI}_4$  were obtained on a Bausch, Lomb/Shimadzu Spectronic 210 UV Spectrophotometer using quartz cells of one centimeter path-length. 8000 Å to 3000 Å were scanned at 500 Å per minute using DMSO, pyridine, and  $\text{H}_2\text{O}$  as solvents. Sublimed films and covalently-

attached dye on glass and  $\text{SnO}_2$  were also studied at the same scan rate and wavelength range (43).

### Electrochemical Studies

Fluoride doped  $\text{SnO}_2$  on 0.38 inch thick glass was manufactured by Pittsburg Plate Glass Co. Sheet titanium metal was obtained from Timet to produce  $\text{TiO}_2$  electrodes. After being cut, polished, and cleaned the Ti electrodes were oxidized by heating red hot, then partially reduced by passing nitrogen gas over them in a muffle furnace for fifteen minutes (54). This gave doped  $\text{TiO}_2$  films having surface resistances between  $500\ \Omega$  and  $1.5\text{k}\Omega$  per square. The thickness of the  $\text{SnO}_2$  films varied between  $5000\ \text{Å}$  and  $7000\ \text{Å}$ . The electrodes were cleaned in an ultrasonic bath, followed by successive washing with Alconox detergent, ethanol, and distilled Milli Q water. The electrodes were then vacuum dried and stored in the glove box.

The solid state potentiostat was of conventional design. The capacitance determination apparatus included a PAR 126 lock-in amplifier, Tektronix oscilloscope, Krohn-Hite 5200 waveform generator, and Fluke digital voltmeter. Capacitance measurements of the electrodes were made by the method of Gileadi and co-workers (44). A twenty-five millivolt amplitude triangular wave of between 100Hz and 1KHz was superimposed on a slowly changing, linear ramp potential. Calibration of output current response was made by means of an external circuit. Compensation for the iR drop between the

reference and the working electrode was made by positive feed back to the control amplifier of the potentiostat.

The basic cell design used for the capacitance and electrochemical studies allowed for sandwich-like positioning of the semiconductor film electrode to the cell body (45). The cells were made of telfon or Lucite for DMSO and  $H_2O$ , respectively, and had a volume of approximately 5 ml. The auxiliary electrode was platinum wire and the reference electrode was Ag wire for DMSO studies and an isolated Ag/AgCl electrode for  $H_2O$  studies.

Solutions were deoxygenated by either of two methods:

- (1) Bubbling with dry, purified nitrogen for 45 minutes.
- (2) Pumping in vacuo with stirring for five minutes then flushing with dry, purified nitrogen, these two steps being repeated several times (46).

Cyclic voltammetric studies of CuPc in the solution, adsorbed, and covalently-attached state were done in DMSO and  $H_2O$ . Solution studies of  $CuPc(SO_3^-Na^+)_4$  were carried out using  $SnO_2$ ,  $TiO_2$ , and platinum as the working electrode. CuPc was sublimed onto  $SnO_2$  at  $5 \times 10^{-5}$  torr. The optimum time was fifteen minutes at 250-270°C, after which the electrodes were cooled and stored in a nitrogen atmosphere (47). This procedure gave defined area, nonporous films of CuPc 20-100 monolayers thick.

### Covalent Attachment

Covalent attachment of CuPc to  $SnO_2$  and  $TiO_2$  was done

using two derivatives of CuPc. The  $\text{SnO}_2$  and  $\text{TiO}_2$  electrodes were silanated using gamma-aminopropyl-triethoxysilane, N, beta-aminoethyl-gamma-aminopropyl-trimethoxysilane or mercapto-propyl-trimethoxysilane. The electrodes were refluxed in a 1% to 5% silane-dry toluene solution under nitrogen for twelve hours after which the excess silane was removed by refluxing the electrodes in dry toluene for one hour (13). The silanated electrodes were stored in dry toluene in the glove box. CuPc was covalently attached to the silanated semiconductors via a sulfonamide formation using  $\text{CuPc}(\text{SO}_3^- \text{Na}^+)_4$  and a thiol formation using  $\text{CuPcI}_4$ .

#### Sulfonamide Attachment

0.1 g  $\text{CuPc}(\text{SO}_3^- \text{Na}^+)_4$ , 20 ml thionyl chloride, 20 ml dry benzene, and 2 drops dimethylformamide were refluxed with stirring for forty-eight hours under nitrogen. The dye was then filtered and washed with dry benzene until the filtrate gave a negative AgCl test. The silanated  $\text{SnO}_2$  and  $\text{TiO}_2$  electrodes, 0.1 g  $\text{CuPc}(\text{SO}_2\text{Cl})_4$ , and 100 ml dry benzene were refluxed under nitrogen for seventy-two hours (48). The chemically-modified electrodes were washed in a Soxhlet extractor with benzene and water for six hours each, vacuum dried, and stored in a nitrogen atmosphere.

#### Thiol

100 ml of  $1 \times 10^{-3} \text{M}$   $\text{CuPcI}_4$  in pH 7 buffer ( $\text{KH}_2\text{PO}_2, \text{NaOH}$ ) was reacted with the silanated semiconductor electrodes at

25-30°C under nitrogen for ten to twelve hours. The chemically-modified electrodes were then washed in Soxhlet extractor with water for twenty-four hours, vacuum dried, and stored under nitrogen.

### Photocurrent Studies

Photocurrent responses of the adsorbed and covalently-attached dye-semiconductor electrodes were studied in DMSO and H<sub>2</sub>O. The studies were done at wavelengths corresponding to the absorptions of the semiconductors (below 350nm and below 400nm for SnO<sub>2</sub> and TiO<sub>2</sub>, respectively) and for the dye (665nm, 630nm). Also, sensitizing agents such as hydroquinone and sodium oxalate were added to the solvents, and photocurrent studies carried out (2). The experimental apparatus included a Electra Powerpac Corp. power supply, 450W or 1000W xenon arc lamp, PAR lock-in amplifier, chopper, Jobin Yvon monochromator or colored filters, Tektronix oscilloscope, and lab-built potentiostat.

### ESCA Analysis

Adsorbed and covalently-attached dye-SnO<sub>2</sub> electrodes, from the electrochemical studies, were used for ESCA analysis. Electrodes biased at different potentials past the various redox peaks of the dye or combinations of peaks as well as unused electrodes were analyzed. All manipulations of the electrodes following the studies were done in a glove box under purified, dry nitrogen. The electrodes were rinsed

thoroughly with ethanol, vacuum dried, and then mounted onto appropriate holders for the surface analysis.

The ESCA data were obtained using a Physical Electronics, Inc. (PHI) Model 548 ESCA/Auger Spectrometer which was equipped with a Mg source ( $\text{Mg K}\alpha_{1,2}$ ). The Mg x-ray beam was operated at a power of 400W. The pressure in the analyzer chambers was maintained at less than  $10^{-9}$  torr during analysis. Binding energies of the ESCA transitions were corrected for charging effects by refering to the  $\text{Sn}(3d_{5/2})$  line of standard  $\text{SnO}_2$ , 486.2ev (49).

Data acquisition, storage, and processing, particularly for obtaining signal averaged ESCA spectra, were accomplished using a NOVA 800 minicomputer (Data General Corporation) which was equipped with 32 K core of memory, 2 Diablo disk (1.2 M bits) and x-y plotting facilities.

Part of the ESCA spectra were "deconvoluted" into separated spectral components. They were computer-simulated by inputting the following parameters: (1) slope of the linear spectral background; (2) the binding energy of each component; (3) the full width at half maximum (FWHM) of each component; (4) peak height of each component; and (5) the percentage of Gaussian contribution to the shape of the spectral band. Parameters 3 and 5 were dependent on the pass energy of the analyzer (25ev or 50ev). Thus, parameters 1, 2, 3, and 5 were held constant for each simulation and parameter 4 varied for each component until a "best fit" was attained for the entire spectrum. Each simulated spectrum was also

corrected for the satellite peaks which were present in the PHI instrument (without a monochromatic x-ray source) (50).

CHAPTER III  
RESULTS AND DISCUSSION

## Solution Studies

### Spectrophotometric Studies of $\text{CuPc}(\text{SO}_3^- \text{Na}^+)_4$

Spectrophotometric studies of  $\text{CuPc}(\text{SO}_3^- \text{Na}^+)_4$  in DMSO and  $\text{H}_2\text{O}$  were carried out to determine major absorption bands and their extinction coefficients. The visible spectrum of  $\text{CuPc}(\text{SO}_3^- \text{Na}^+)_4$  in DMSO (Figure 4) shows major transitions at 677nm and 349nm with extinction coefficients of  $1.2 \times 10^5 \text{M}^{-1} \text{cm}^{-1}$  and  $0.4 \times 10^5 \text{M}^{-1} \text{cm}^{-1}$  respectively, corresponding to  $\pi-\pi^*$  transitions of the phthalocyanine ring. The spectrum in water (Figure 4) is different; two bands at 630nm and 665nm ( $E = 6.1 \times 10^4 \text{M}^{-1} \text{cm}^{-1}$  and  $4.4 \times 10^4 \text{M}^{-1} \text{cm}^{-1}$ , respectively) are observed giving a broad absorbance in the 500-700nm spectra region. The spectral band at 336nm appears to correspond to a shift of the 349nm band in DMSO, with little change in its extinction coefficient. Association or self-solvation of  $\text{CuPc}(\text{SO}_3^- \text{Na}^+)_4$  in water is implied by the presence of the broad 630, 655nm doublet (51).

### Electrochemistry of $\text{CuPc}(\text{SO}_3^- \text{Na}^+)_4$

The electrochemical reactions of  $\text{CuPc}(\text{SO}_3^- \text{Na}^+)_4$  were explored by cyclic voltammetry in DMSO and  $\text{H}_2\text{O}$  to determine the position of each redox level of the dye with respect to the conduction and valence bands of  $\text{SnO}_2$  and  $\text{TiO}_2$ . The aim was to probe the relation between the band structure and reactivity of solution species and map the band gap region of the semiconductors to determine the presence and energies of any

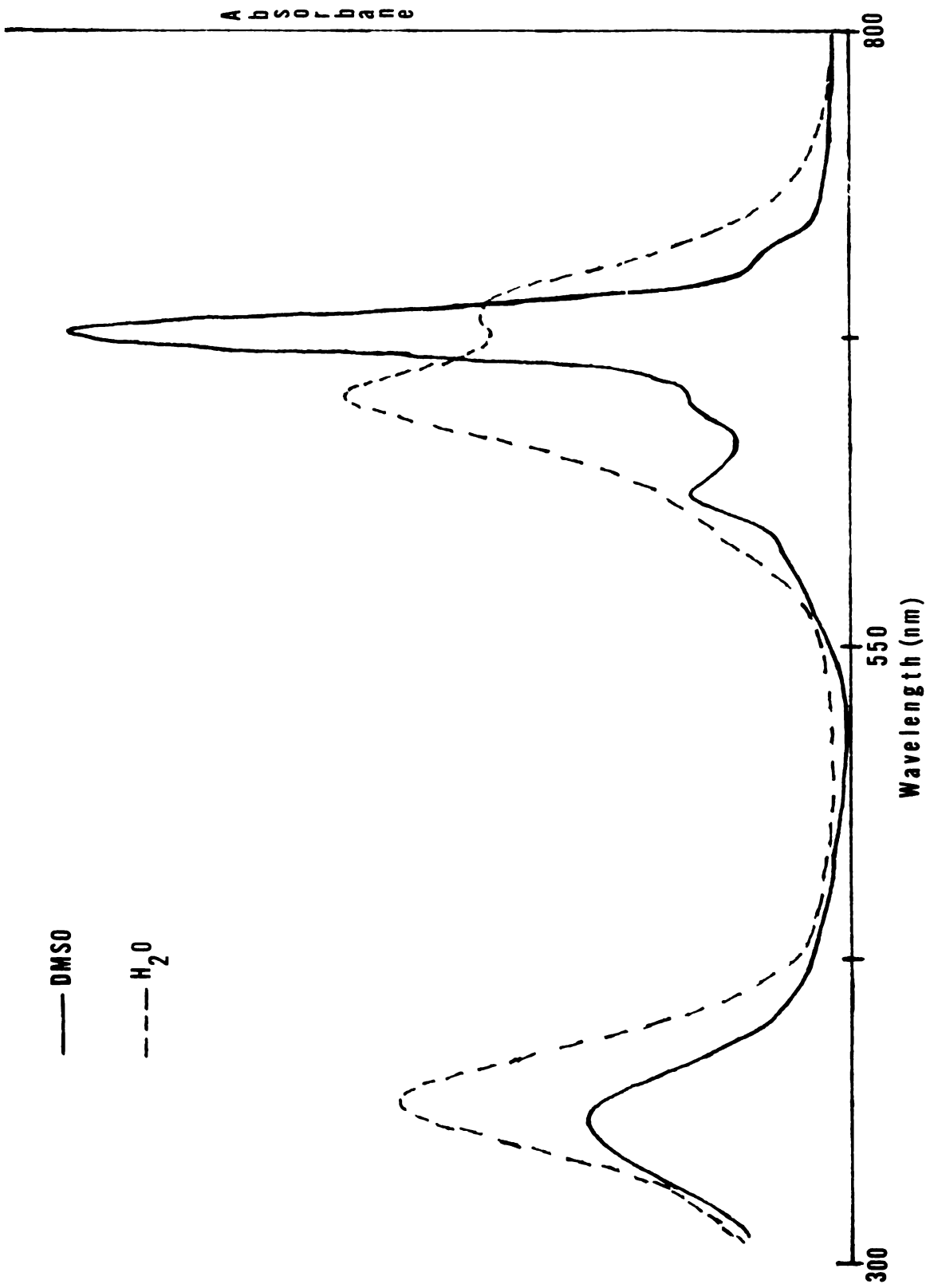


Figure 4. Absorption spectra of  $\text{CuPc}(\text{SO}_3\text{Na}^+)_4$  in DMSO and  $\text{H}_2\text{O}$ .

intermediate bands or surface states.

The cyclic voltammetric behavior of  $\text{CuPc}(\text{SO}_3^- \text{Na}^+)_4$  in DMSO at highly-doped  $\text{SnO}_2$  and  $\text{TiO}_2$  electrodes as well as platinum is shown in Figure 5. Redox couples a/a' and b/b' correspond to the formation and reoxidation of the mono and dianion forms of CuPc (30). The two one-electron processes are nearly reversible on a platinum electrode ( $\Delta E_{\text{peak}} < 100\text{mv}$  for  $v < 100\text{mv/sec}$ ) and have been attributed to addition of electrons to the phthalocyanine ring and not the reduction of copper (31). These processes appear to be slightly less reversible on  $\text{SnO}_2$  ( $\Delta E_{\text{peak}}$  larger at the same scan rate). Redox couples a/a' and b/b' are poorly resolved and appear even less chemically (i.e. slightly disproportional peak current ratios) reversible on  $\text{TiO}_2$ ; a/a' is also obscured by a desorption process.

Redox couple c/c' corresponds to the formation of the monocation form of CuPc and its reduction. The cyclic voltammetric studies indicate that the oxidation is followed by a slow chemical reaction. The peak current ratio  $i_{\text{pc}}/i_{\text{pa}}$  for this process approaches 1.0 on  $\text{SnO}_2$  electrodes as the scan rate is increased. This redox couple appears to be more chemically reversible on  $\text{SnO}_2$  than on platinum or  $\text{TiO}_2$ . An explanation for this will be given in a later section.

Redox couples d/d' and e/e' are unexplained reductions which do not appear very well resolved unless an anodic scan has been performed previously. The trianion of CuPc has been formed via sodium reduction (52); it is possible redox couple

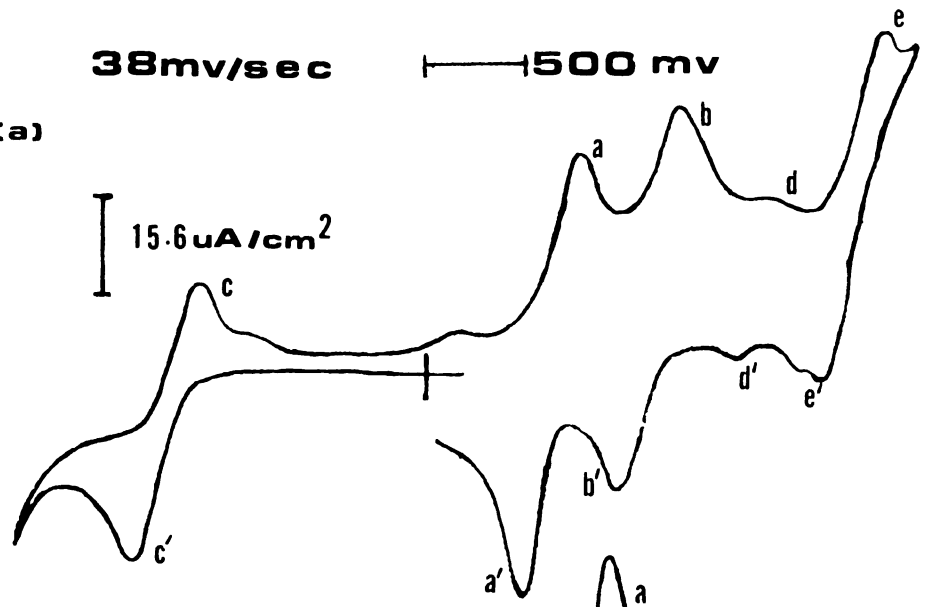
Figure 5. Cyclic voltammetry of  $\text{CuPc}(\text{SO}_3^- \text{Na}^+)_4$  in  $0.1 \mu\text{M}$  TEAP/DMSO at (a)  $\text{SnO}_2$ , (b)  $\text{TiO}_2$  and (c) Pt.

38mv/sec

500 mv

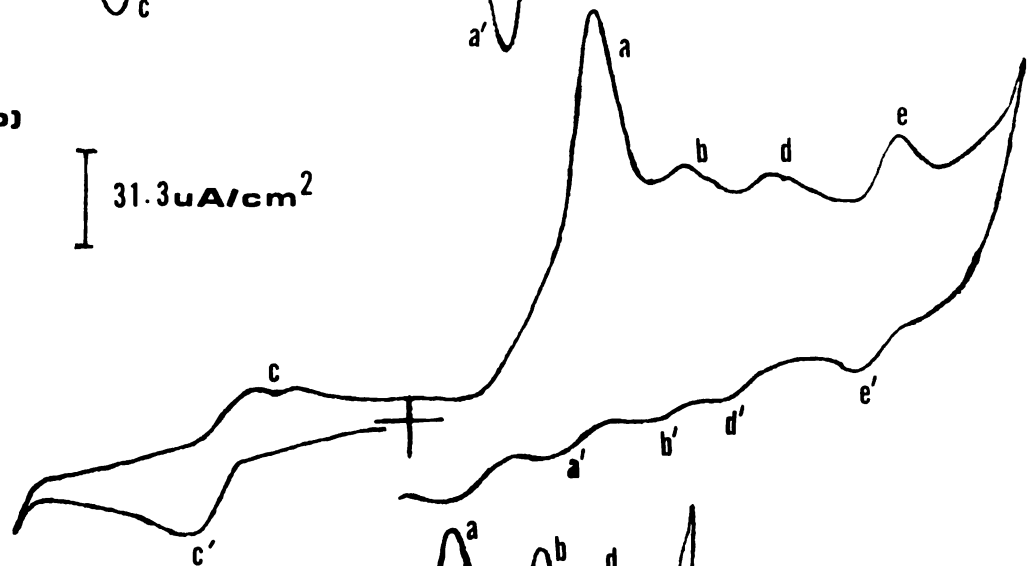
(a)

15.6  $\mu\text{A}/\text{cm}^2$



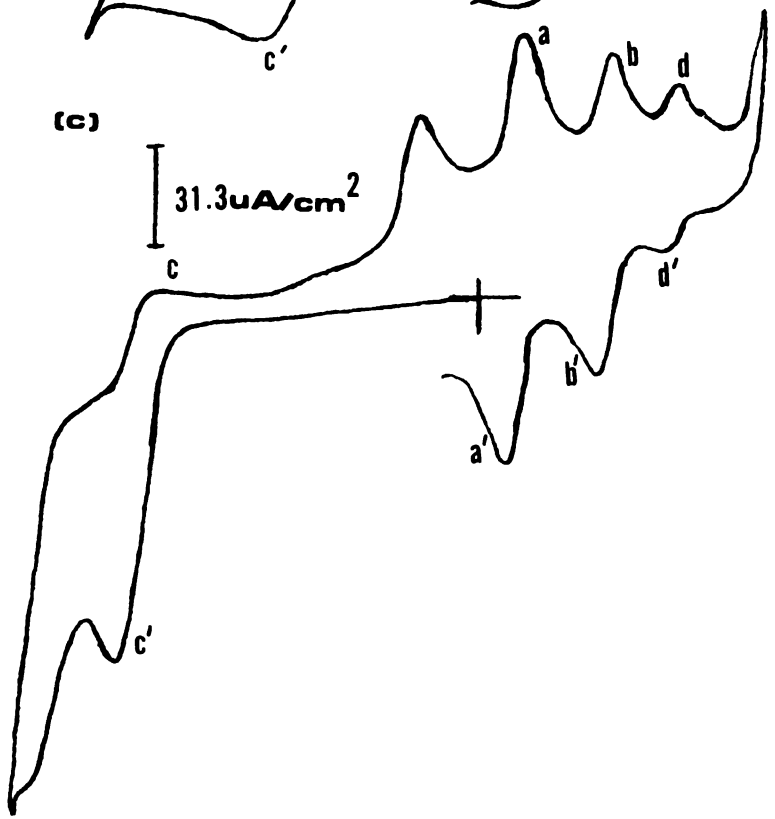
(b)

31.3  $\mu\text{A}/\text{cm}^2$



(c)

31.3  $\mu\text{A}/\text{cm}^2$



d/d' is the formation and reoxidation of the trianion. It is also conceivable that one of these couples correspond to the reduction of the product of the chemical reaction consuming the oxidative intermediate of  $\text{CuPc}(\text{SO}_3^-\text{Na}^+)_4$ . These redox couples are not resolved as well from the background currents on  $\text{SnO}_2$  as on  $\text{TiO}_2$  or Pt.

The cyclic voltammetric behavior of  $\text{CuPc}(\text{SO}_3^-\text{Na}^+)_4$  in  $\text{H}_2\text{O}$  (pH 4) was found to be more complicated than in DMSO (Figure 6). Two poorly resolved reduction peaks were observed on  $\text{SnO}_2$  at -0.8 volts and -0.93 volts vs Ag/AgCl. The reductions appeared chemically irreversible, and anodic wave was observed on the return scan at -0.1 volts corresponding to the oxidation of products formed on the cathodic sweep. These reductions were less resolved on  $\text{TiO}_2$ . A very poorly defined oxidative wave was observed at 1.0 volts and 1.2 volts vs Ag/AgCl for  $\text{SnO}_2$  and  $\text{TiO}_2$ , respectively, which was chemically irreversible.

The difference in electrochemical behavior of  $\text{CuPc}(\text{SO}_3^-\text{Na}^+)_4$  in DMSO and  $\text{H}_2\text{O}$  probably results from the difference in the chemical state of  $\text{CuPc}(\text{SO}_3^-\text{Na}^+)_4$  in both solvents, the stability of the redox intermediates in both solvents, and the state of the semiconductor surface in both solvents. An associated form of  $\text{CuPc}(\text{SO}_3^-\text{Na}^+)_4$  in  $\text{H}_2\text{O}$  may inhibit charge transfer; the irreversible electrochemical behavior in  $\text{H}_2\text{O}$  was not surprising (51).

A differential capacitance plot of  $1/C_{sc}^2$  vs potential according to the Mott-Schottky equation

$$1/C_{sc}^2 = 2/\epsilon\epsilon_0 e_0 n_0 \phi_s - kT/e_0$$

yields information about the effective carrier density  $n_0$  from

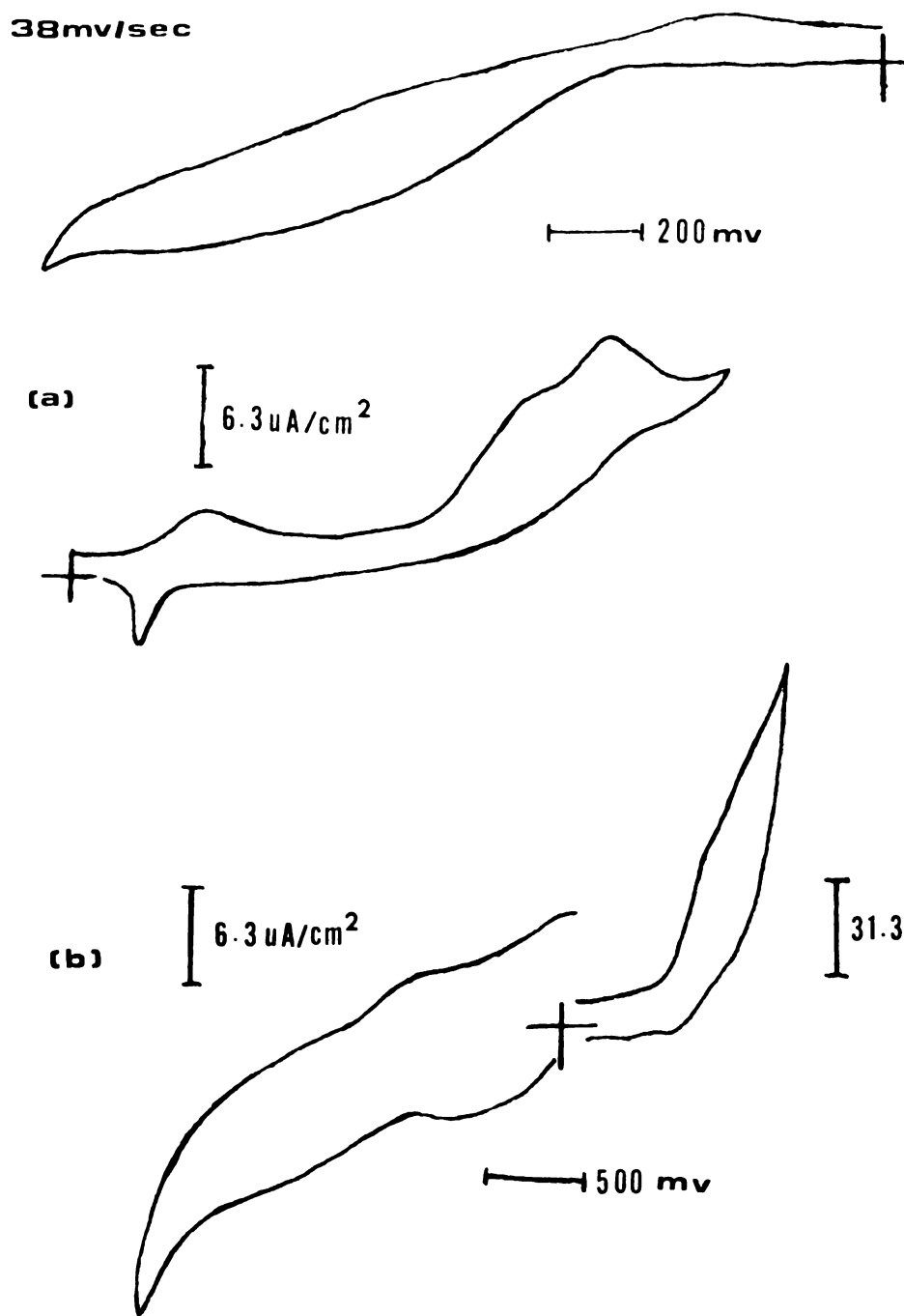


Figure 6. Cyclic voltammetry of  $\text{CuPc}(\text{SO}_3^- \text{Na}^+)_4$  in  $\text{H}_2\text{O}$  (pH 4) at (a)  $\text{SnO}_2$  and (b)  $\text{TiO}_2$ .

the slope of the plot and the flatband potential  $V_{fb}$  from the potential axis intercept. The results of these measurements for  $\text{SnO}_2$  and  $\text{TiO}_2$  in DMSO and  $\text{H}_2\text{O}$  are shown in Figures 7 and 8. The effective carrier densities, assuming dielectric constants of 12.5 and 127 for  $\text{SnO}_2$  and  $\text{TiO}_2$ , respectively, were as follows:  $-1.65 \pm 0.1$  volts vs AgRE ( $\text{SnO}_2/\text{DMSO}$ ),  $-1.43 \pm 0.1$  volts vs Ag/AgCl ( $\text{SnO}_2/\text{H}_2\text{O}$ ),  $-2.0 \pm 0.1$  volts vs AgRE ( $\text{TiO}_2/\text{DMSO}$ ), and  $-1.4$  volts vs Ag/AgCl ( $\text{TiO}_2/\text{H}_2\text{O}$ ). From the donor density, flatband potentials and band gaps of  $\text{SnO}_2$  and  $\text{TiO}_2$  (3.5eV and 3.0eV, respectively) the energy positions of the valence band and conduction band edges ( $E_v$  and  $E_c$ ) are determined from the relation

$$E_c(\text{eV}) = e_0 V_{fb} + kT \ln (n_0/N_c)$$

where  $N_c$  the density of states at the bottom of the conduction band is about  $10^{-19}$  carriers  $\text{cm}^{-3}$  in most semiconductors (53).

Figures 9 and 10 show the relation between the band structures of the semiconductors and the redox couples of  $\text{CuPc}(\text{SO}_3^- \text{Na}^+)_4$  in DMSO and  $\text{H}_2\text{O}$ . The reductions and oxidation of  $\text{CuPc}(\text{SO}_3^- \text{Na}^+)_4$  occur at potentials coincident with the band gap region of  $\text{SnO}_2$  and  $\text{TiO}_2$ . The fact that the processes appear chemically reversible or pseudo-reversible in DMSO may indicate the contribution of surface states to the charge transfer process or electron tunneling through the narrow depletion region since the number of charge carriers is high. Surface states can be thought of as intermediate energy levels of narrow width in the band gap region. Adsorbed species or surface defects of the semiconductor generate these surface states

Figure 7. Differential capacitance vs potential plots of  $\text{SnO}_2$  in  $0.1\mu$  TEAP/DMSO and  $\text{H}_2\text{O}$ (pH 4).

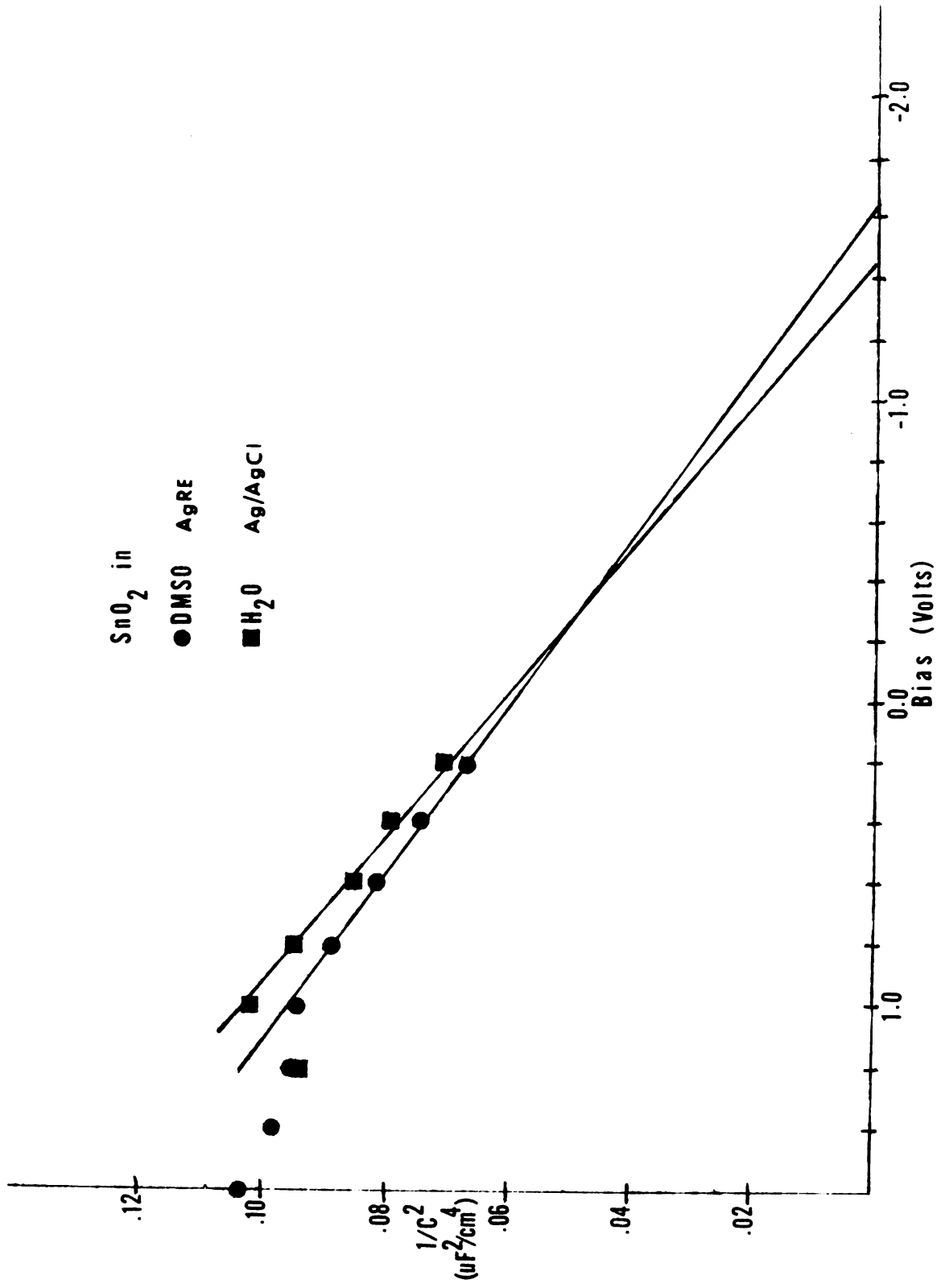


Figure 4. Differential capacitance vs potential plots of  $\text{TiO}_2$  in  $0.1 \mu\text{M}$  TEAP/DMSO and  $\text{H}_2\text{O}$  (pH 4).

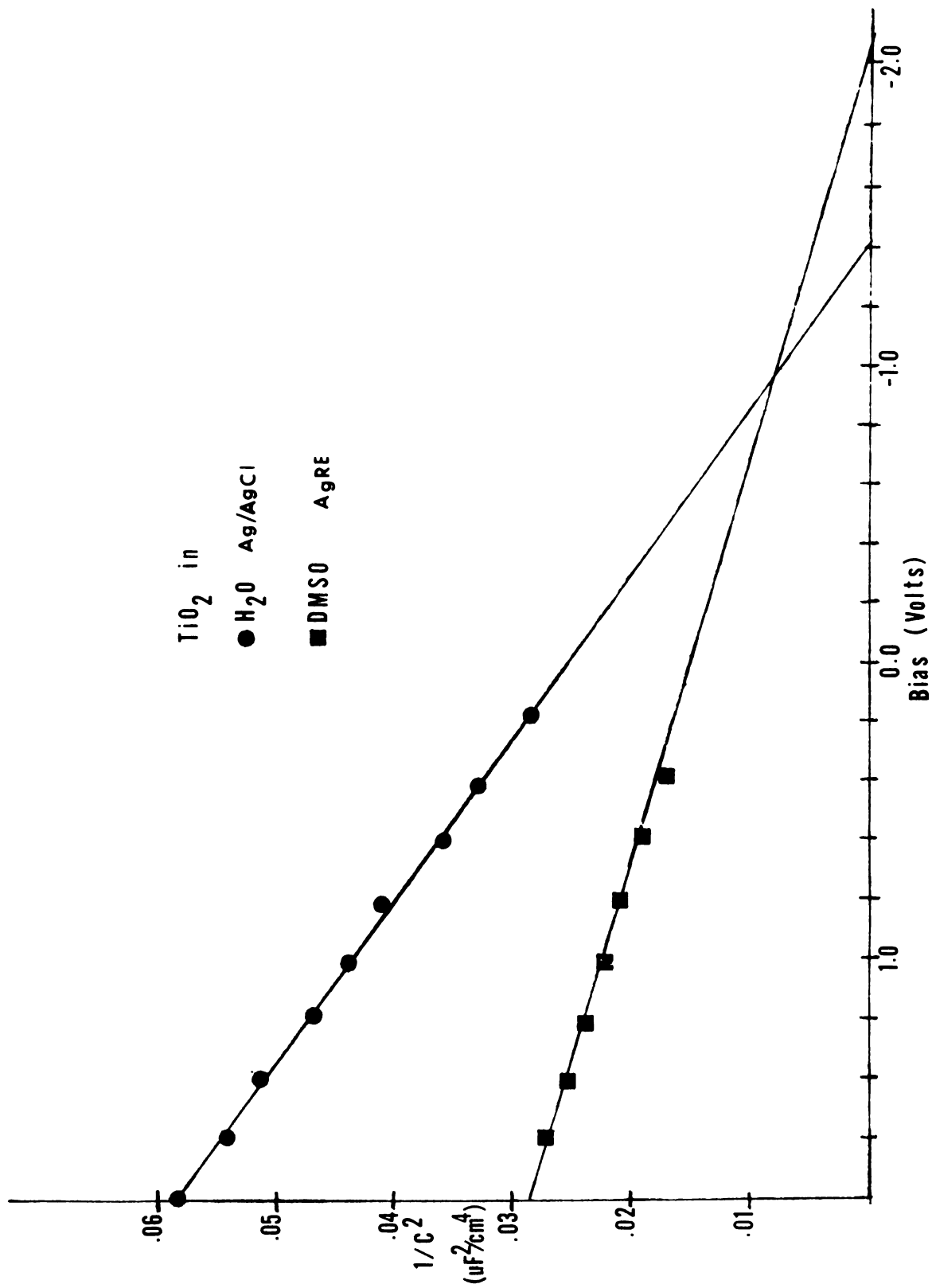
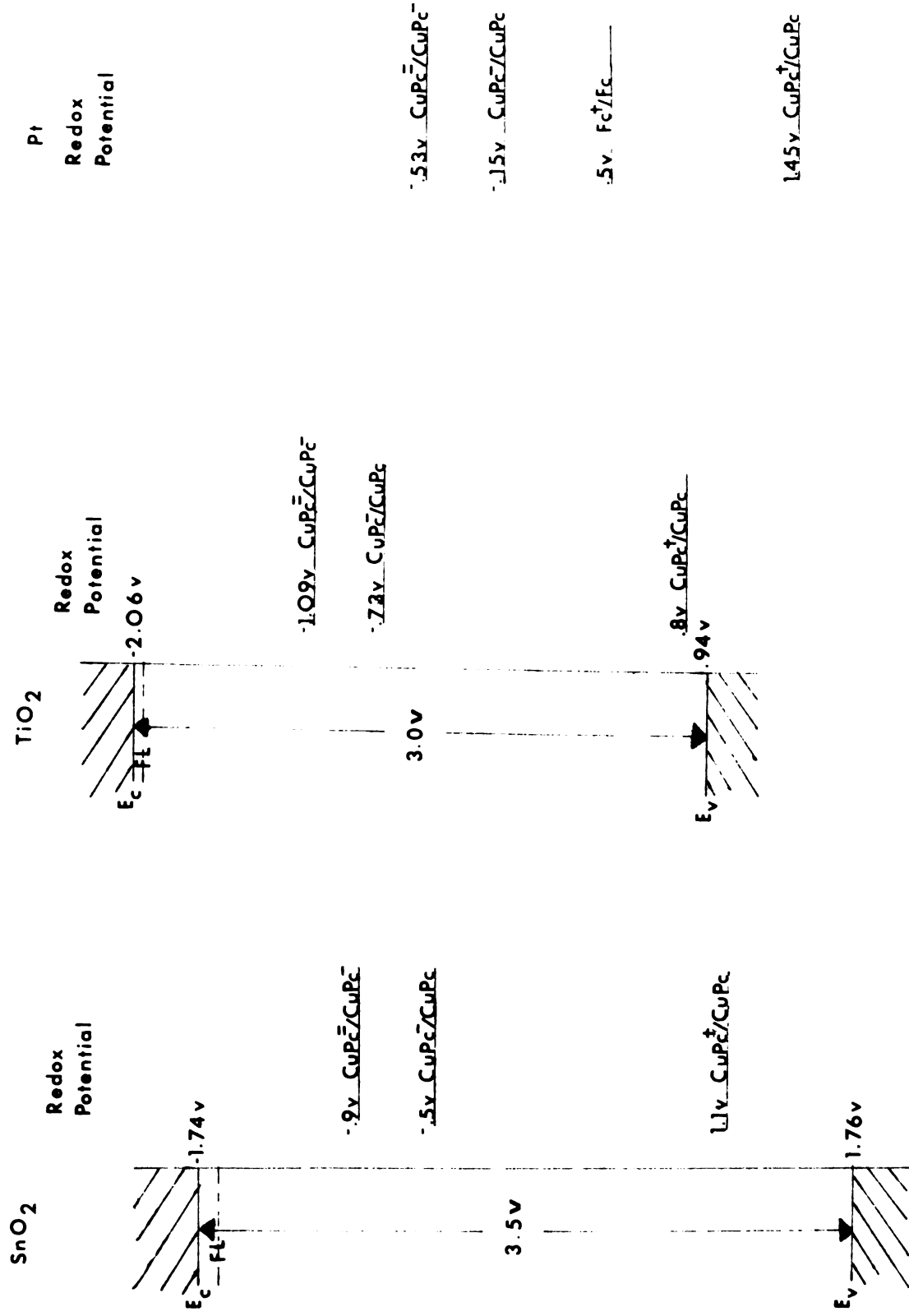


Figure 9. Energy diagram of  $\text{CuPc}(\text{SO}_3^- \text{Na}^+)_4$  redox couples in  $0.1 \mu\text{ TEAP/DMSO}$  at  $\text{SnC}_2$ ,  $\text{TiO}_2$  and Pt. Ferrocene (Fc) at Pt is given for reference.



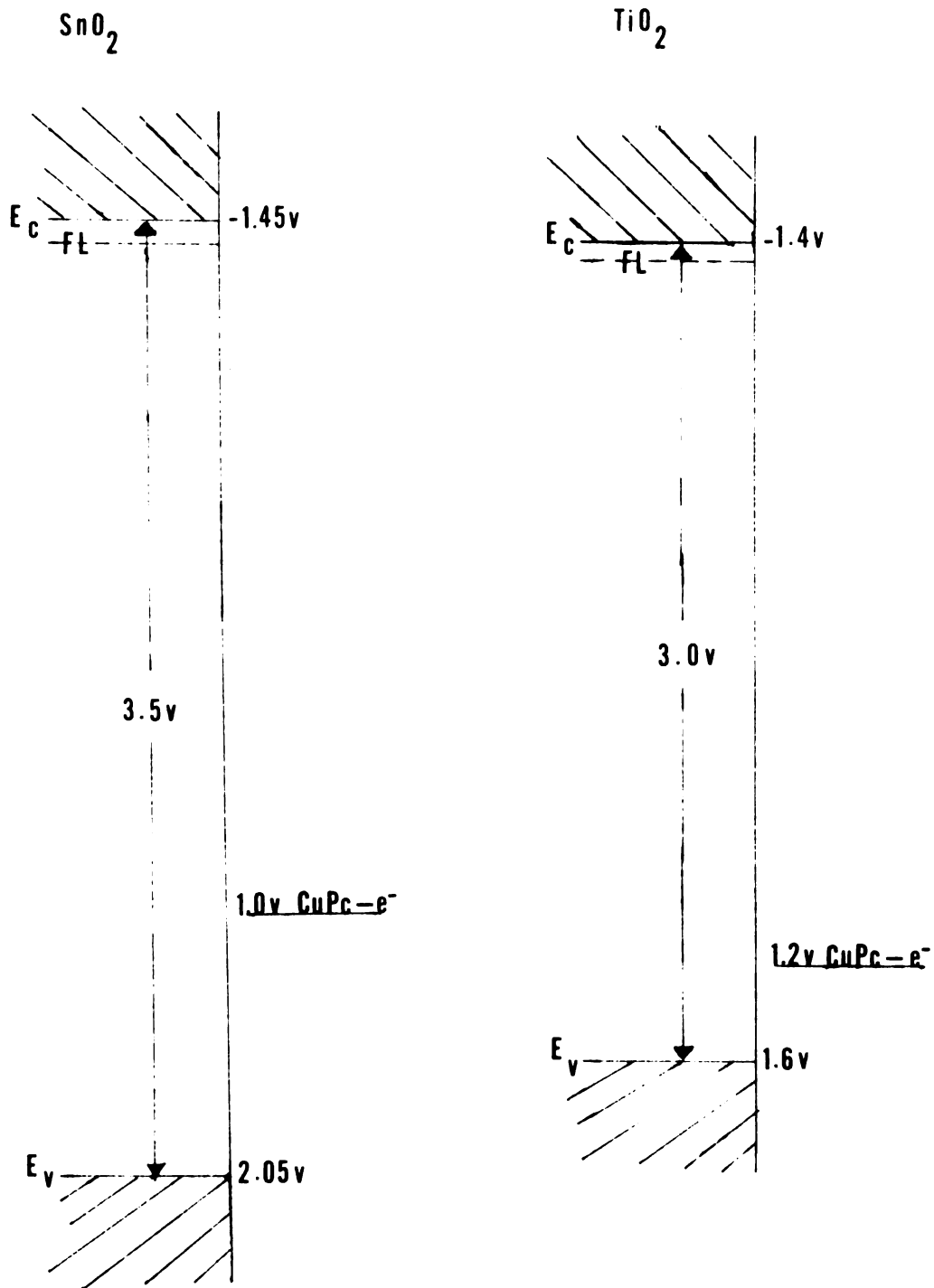


Figure 10. Energy diagram of  $\text{CuPc}(\text{SO}_3^- \text{Na}^+)_4$  oxidation in  $\text{H}_2\text{O}$  (pH 4) at  $\text{SnO}_2$  and  $\text{TiO}_2$ .

through which electron transfer can occur. As the carrier concentration increases, the charge depletion region at the surface decreases in thickness. When the carrier density is sufficiently high enough, this depletion thickness will be  $10 \text{ \AA}^{\circ}$  or less, which enables electron tunneling to occur (54). The redox couples of the dye and ferrocene in DMSO at platinum are shown in Figure 9 for reference.

The redox couples at  $\text{SnO}_2$  and  $\text{TiO}_2$  are shifted cathodically from the potential at which they occur at platinum. When the number of charge carriers at the electrodes surface approaches  $N_c$ , degeneracy begins and electrode behavior becomes more metal like. Thus, the higher the carrier density, the more metal-like a semiconductor electrode's behavior is, i.e. reductions of  $\text{CuPc}(\text{SO}_3^- \text{Na}^+)_4$  occur at cathodic potentials closer to potentials corresponding to the reductions at platinum (8). The couples at  $\text{SnO}_2$  are shifted less and the carrier density higher indicating the  $\text{SnO}_2$  is more metal-like than the  $\text{TiO}_2$ .

### Adsorbed Dye Studies

#### Spectrophotometric Studies of CuPc on $\text{SnO}_2$

An absorption spectra of copper phthalocyanine (CuPc) deposited on  $\text{SnO}_2$  is shown in Figure 11. Absorption maxima occur at 694nm and 620nm in comparison to 691nm and 624nm for CuPc deposited on glass (29). The spectra indicated the films to be in the  $\alpha$  form. The CuPc thin films could be vacuum deposited on the  $\text{SnO}_2$  surface in one of three ways:

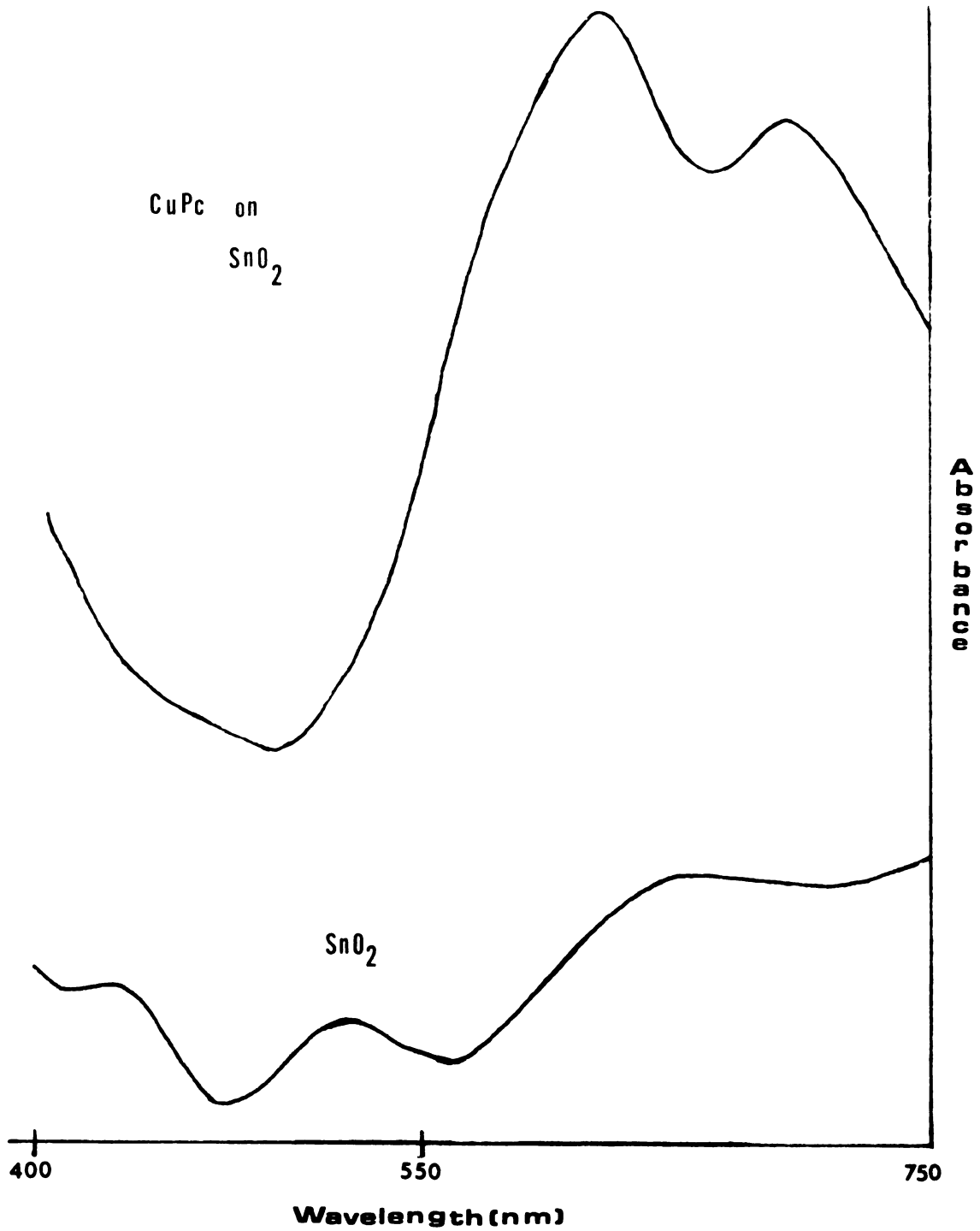


Figure 11. Absorption spectra of clean SnO<sub>2</sub> and CuPc sublimed on SnO<sub>2</sub> electrodes.

with the crystallites parallel with the surface, with the crystallites standing obliquely to it, or some combination of these two arrangements (63). Assuming an electrode area of  $0.8 \text{ cm}^2$ , a dye diameter of  $14.3 \text{ \AA}$ , and an extinction coefficient of  $3.32 \times 10^4 \text{ M}^{-1} \text{ cm}^{-1}$  at  $618 \text{ nm}$  (27), one could determine the approximate thickness of the films from Beer's Law ( $A = bc$ ). The  $\text{SnO}_2$  contribution to the adsorption at  $618 \text{ nm}$  was subtracted before calculating the thickness of the films. This method resulted in films varying between 20-100 monolayers with  $3.91 \times 10^{13}$  molecules per monolayer.

#### Electrochemistry of CuPc on $\text{SnO}_2$

The electrochemistry of CuPc sublimed on  $\text{SnO}_2$  in DMSO is shown in Figure 12. Cathodic scans showed the first reduction wave (1) at  $-0.75$  volts vs AgRE, shifted  $0.13$  volts cathodically from the peak potential of the solution component (Figure 5). Scanning back anodically resulted in an oxidation wave (2) at  $1.4$  volts vs AgRE. Both waves appeared chemically irreversible. Upon scanning to the second reduction peak (3) potential, a large symmetrical desorption current peak was observed, coincident with the visible loss of CuPc from the electrode surface. Returning anodic scans indicated the reversible oxidation of the two reduction intermediates, ( $3', 1'$ ) but a resorption process wasn't observed. If the potential was cycled repeatedly between the cathodic and anodic limits, the desorption occurring at the second cathodic peak potential slowly decayed away, the oxidation wave

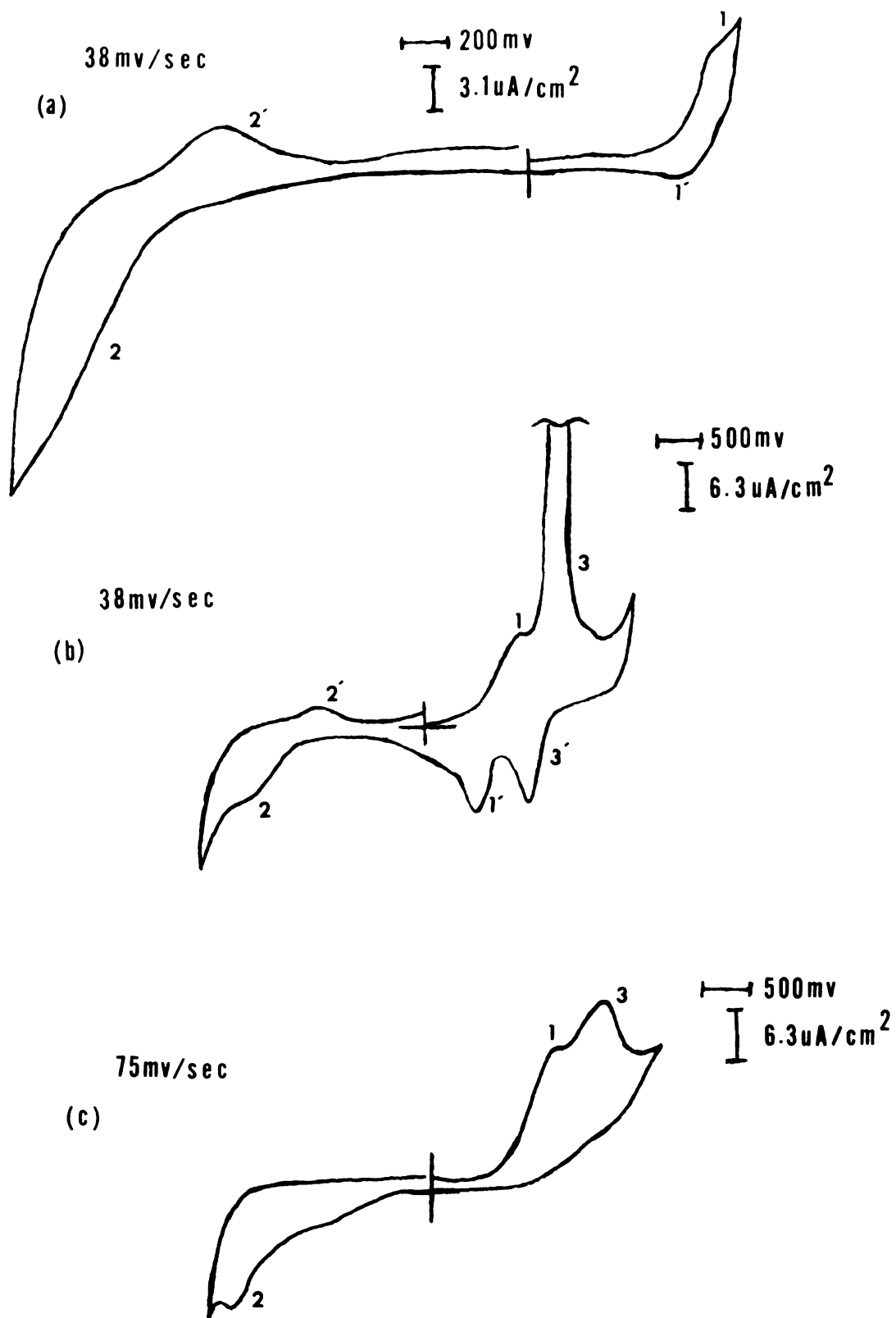


Figure 12. Cyclic voltammetry of CuPc sublimed on  $\text{SnO}_2$  in  $0.1 \mu$  TEAP/DMSO.

(2) and two reduction waves (1,3) retained a constant magnitude indicating the fact that some of the dye remained after the desorption process and was electrochemically active. All three peaks appeared to be chemically irreversible, i.e. disproportional peak current ratios.

These electrochemical experiments indicate that the sublimation process produces a tightly-bound form of dye and a loosely-held form which can be desorbed at a potential very near the second reduction. The formation of the dianion species may force this desorption. If the dye remained purely surface bound at all potentials, electron transfer to and from it should occur with symmetrical reduction and oxidation peaks with a  $\Delta E_{\text{peak}}$  near zero. Oxidation of the reduction intermediates should be diffusion controlled since they were still near the electrode surface immediately after being desorbed. Diffusion control is indicated by the cyclic behavior observed, i.e.  $\Delta E_{\text{peak}} \approx 100\text{mv}$ .

The cyclic voltammetric studies of CuPc sublimed on  $\text{SnO}_2$  in  $\text{H}_2\text{O}$  resulted in poorly defined and irreversible reduction and oxidation processes. No desorption of the dye was observed during the scans in any aqueous media.

#### ESCA of CuPc on $\text{SnO}_2$

To facilitate the understanding of the adsorbed CuPc/ $\text{SnO}_2$  electrochemistry, ESCA analysis of electrodes in various states of pretreatment along with standards was carried out. Changes in surface concentration and valence states of the

adsorbed dye occurring as a result of these electrochemical pretreatments are easily observed with ESCA. The Cu( $2p_{1/2}, 3/2$ ) ESCA spectra are shown in Figure 13. Since SnO<sub>2</sub> was a common component for all these materials, the binding energies of all components were corrected to the Sn( $3d_{5/2}$ ) line of standard SnO<sub>2</sub>, 486.2ev (49). The Cu( $2p_{1/2}, 3/2$ ) peaks except for spectrum (g)(H<sub>2</sub>O) are accompanied by multiplets at binding energies approximately 9-10 ev higher than the 2p transitions. This type of multiplet splitting has been previously reported for metal (paramagnetic) oxides. This splitting has been contributed to the presence of oxygen in the oxide lattice (SnO<sub>2</sub>), adsorbed oxygen, or another oxygen containing molecule (55). Binding energies of the Cu( $2p_{3/2}$ ) and Cu(Auger) peaks for the various samples are given in Table 1. Because there is little binding energy shift in the Cu ( $2p_{1/2}, 3/2$ ) peaks for the various copper species, the most useful information can be obtained from the Cu( $2p_{3/2}$ ) - Cu (Auger) binding energies. This binding energy difference does shift with a change in the copper valence state. CuPc/SnO<sub>2</sub> pressed pellet, CuPc/SnO<sub>2</sub> unused electrode, and CuPc/SnO<sub>2</sub> electrode (DMSO)  $\Delta$ BE's (597.1ev, 596.8ev, and 597.0ev, respectively) correlate well with that of CuO (596.9ev) (57), thus indicating the presence of Cu(II) species. The  $\Delta$ BE for CuSO<sub>4</sub> (anhydrous)/SnO<sub>2</sub> standard pellet is slightly lower, 595.8ev. The absence of multiplet splitting and the BE (594.9ev) for the CuPc/SnO<sub>2</sub> electrode in H<sub>2</sub>O seems to signify the presence of a copper species more reduced than

Figure 13.  $\text{Cu}(2p_{1/2,3/2})$  ESCA spectra of (a)  $\text{CuSO}_4/\text{SnO}_2$  powder pressed pellet, (b)  $\text{CuPc}/\text{SnO}_2$  powder pressed pellet, (c)  $\text{CuPc}/\text{SnO}_2$  unused electrode, (d)  $\text{CuPc}/\text{SnO}_2$  electrode in DMSO (scanned past 1st reduction peak and back anodically to the oxidation peak), (e)  $\text{CuPc}/\text{SnO}_2$  electrode in DMSO (scanned past 2nd reduction peak and back anodically to the oxidation peak), (f)  $\text{CuPc}/\text{SnO}_2$  electrode in DMSO (scanned until desorption process complete), (g)  $\text{CuPc}/\text{SnO}_2$  electrode in  $\text{H}_2\text{O}$  (scanned until desorption process complete).

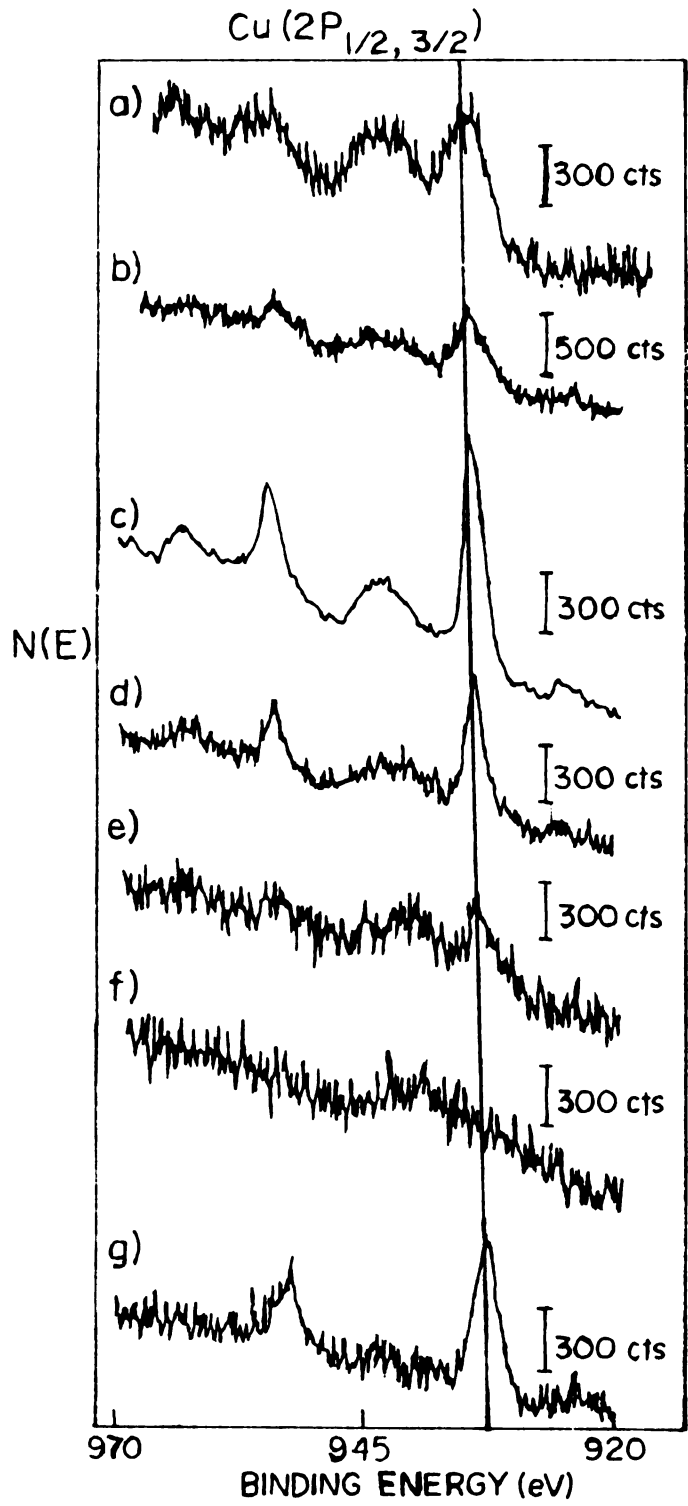


Table 1. ESCA Data CuPc/SnO<sub>2</sub>

Sample	<u>B.E.(Cu(2p<sub>3/2</sub>))</u> (a)	<u>B.E.(Cu(Auger))</u> (a)	<u>Δ B.E.</u> (c)	<u>B.E.(N(1s))</u> (a)	<u>N/C</u> (b)
CuSO <sub>4</sub>	933.7	337.9(916.1)	595.8		
CuPc standard pellet/SnO <sub>2</sub> powder	934.5	337.4(916.1)	597.1	398.0	.46
CuPc/SnO <sub>2</sub> elec- trode unused	934.0	337.2(916.8)	596.8	397.9	.46
CuPc/SnO <sub>2</sub> elec- trode/DMSO	934.1	337.1(916.7)	597.0	397.9	.49
CuPc/SnO <sub>2</sub> elec- trode/H <sub>2</sub> O	932.8	337.9(916.1)	594.9	398.3	
CuO	933.8(d)				
CuO			596.9(e)		
Cu <sub>2</sub> O			596.2(e)		
Cu			595.3(e)		

(a) Corrected to Sn(3d<sub>5/2</sub>) = 486.2eV, Reference (49)

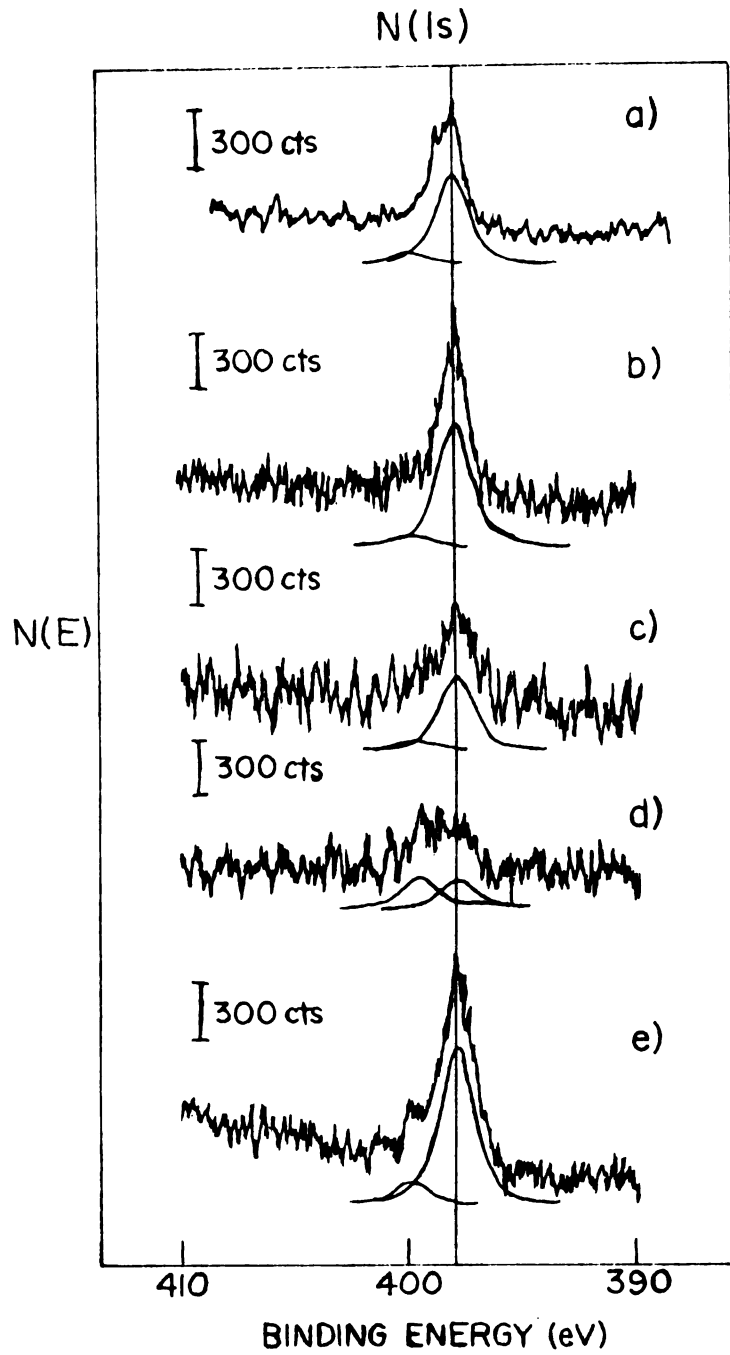
(d) Reference (56)

(b) Corrected for relative XPS sensitivities

(e) Reference (57)

(c) Cu(2p<sub>3/2</sub>) - Cu(Auger) Binding Energies

Figure 14. N(1s) ESCA spectra of (a) CuPc/SnO<sub>2</sub> unused electrode, (b) CuPc/SnO<sub>2</sub> electrode in DMSO (scanned past first reduction peak and back anodically to the oxidation peak), (c) CuPc/SnO<sub>2</sub> electrode in DMSO (scanned past the second reduction peak and back anodically to the oxidation peak), (d) CuPc/SnO<sub>2</sub> electrode in DMSO (scanned until desorption process is complete) and (e) CuPc/SnO<sub>2</sub> electrode in H<sub>2</sub>O (scanned until desorption process is complete).



Cu(II) (57).

N(1s) spectra of the CuPc films consisted of two components, a major peak at 398.0ev and a satellite at 399.7ev (Figure 14) as previously reported (38). After cycling the electrode potential past the second reduction peak, which resulted in a large desorption, the ESCA spectra showed a diminished CuPc surface concentration (Spectrum d). The N(1s) spectrum was then equally divided between the 398.0ev and 399.7ev component, indicating the probably existence of de-metalled phthalocyanine in the films (38). It seems reasonable that the sublimation process could produce a small amount of the de-metalled form of phthalocyanine. Since the Cu(2p<sub>1/2,3/2</sub>) spectrum of this electrode indicated almost no copper present, the de-metalled form was probably deposited first. This new type of phthalocyanine system made up at most approximately 5-10% of the total phthalocyanine film.

#### Photocurrent Response of CuPc on SnO<sub>2</sub>

The dark and light cyclic voltammograms of CuPc deposited on SnO<sub>2</sub> in 0.05M Na<sub>2</sub>C<sub>2</sub>O<sub>4</sub> (supersensitizer or reducing agent as described on page )/pH 7 buffer are shown in Figure 15. Since the photocurrent response corresponded to the absorption spectrum of the CuPc, IR, UV, long pass 470nm, and long pass 540nm filters were used. This combination of filters resulted in a wavelength window in which maximum absorption of the dye occurred (550nm-750nm); it also filtered out any semiconductor response (< 400nm). The photocurrent response appeared to begin at approximately 0.5 volts

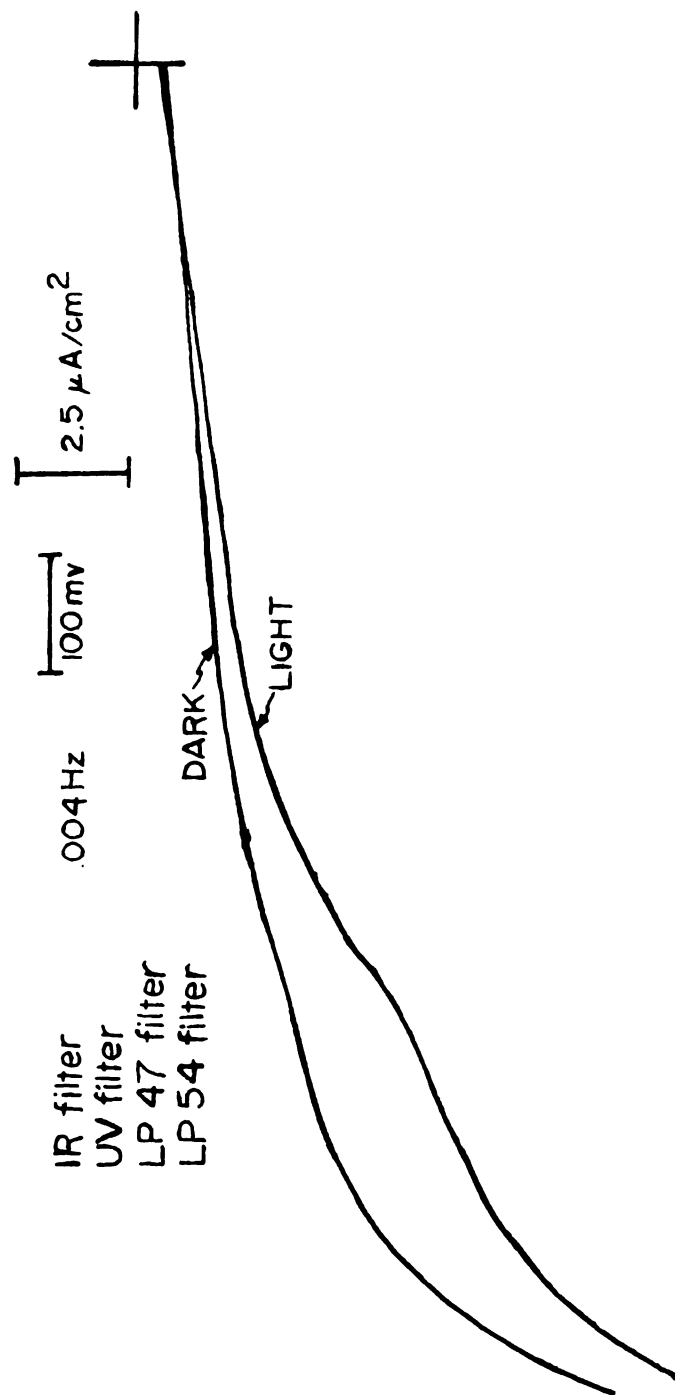


Figure 15. Photocurrent response of a CuPc/SnO<sub>2</sub> electrode in 0.05M Na<sub>2</sub>C<sub>2</sub>O<sub>4</sub>/pH 7 buffer.

vs Ag/AgCl reference. A maximum value of  $1.5 \mu\text{A}/\text{cm}^2$  was obtained at approximately 0.9 volts vs reference after which the photocurrent response decayed back to essentially zero.

In another experiment, the light source was chopped at 13 Hz and the photocurrent measured using the lockin technique. This technique employed the light chopper frequency as a reference for the lockin amplifier, thus allowing easier detection of the electrode photocurrent response. The photocurrent as a function of anodic bias potential was studied. The results for two electrodes having approximately the same dye coverage are shown in Figure 16. Electrode A was biased at 0.2 volts, 0.5 volts, 0.9 volts, then 0.5 volts and 0.2 volts vs Ag/AgCl reference and the photocurrent response recorded. The response appeared to reach a maximum between 0.5 volts and 0.9 volts. The second readouts at 0.5 volts and 0.2 volts were slightly less than the final steady response at 0.9 volts.

The other electrode (B) was biased at 0.9 volts and an initial reading taken. The response decayed over a period of several minutes to a steady photocurrent approximately one-fourth of the initial value. As with electrode A, the photocurrent response at 0.5 volts and 0.2 volts was slightly less than the final steady 0.9 volts response.

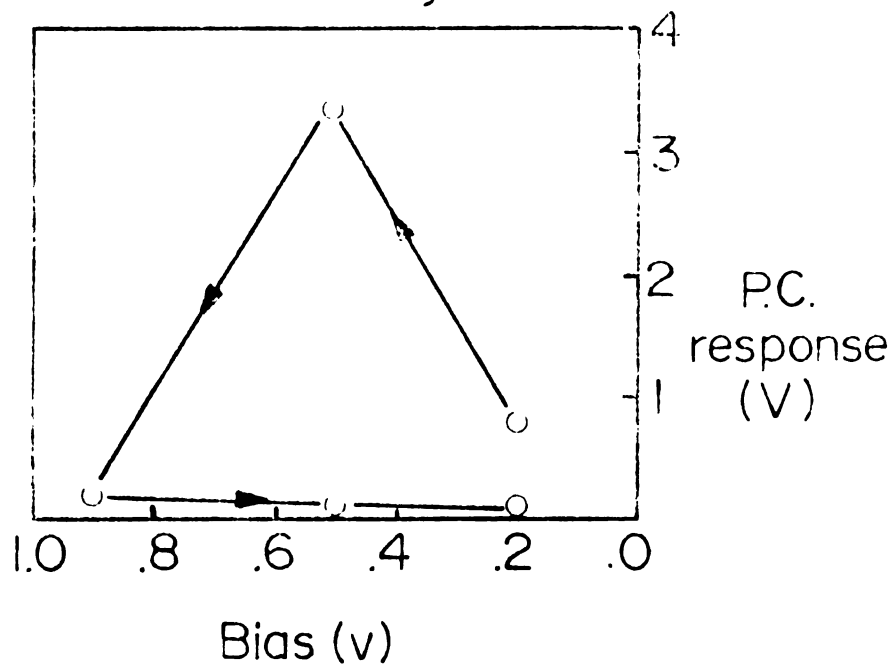
After the photocurrent studies, visual examination of the electrodes indicated partial desorption and/or decomposition of the CuPc film. This phenomenon appeared to be potential dependent; it occurred at potentials anodic of 0.5 volts.

Figure 16. Photocurrent response vs anodic bias potential plots of two CuPc/SnO<sub>2</sub> electrodes in 0.05M Na<sub>2</sub>C<sub>2</sub>O<sub>4</sub>/pH 7 buffer.

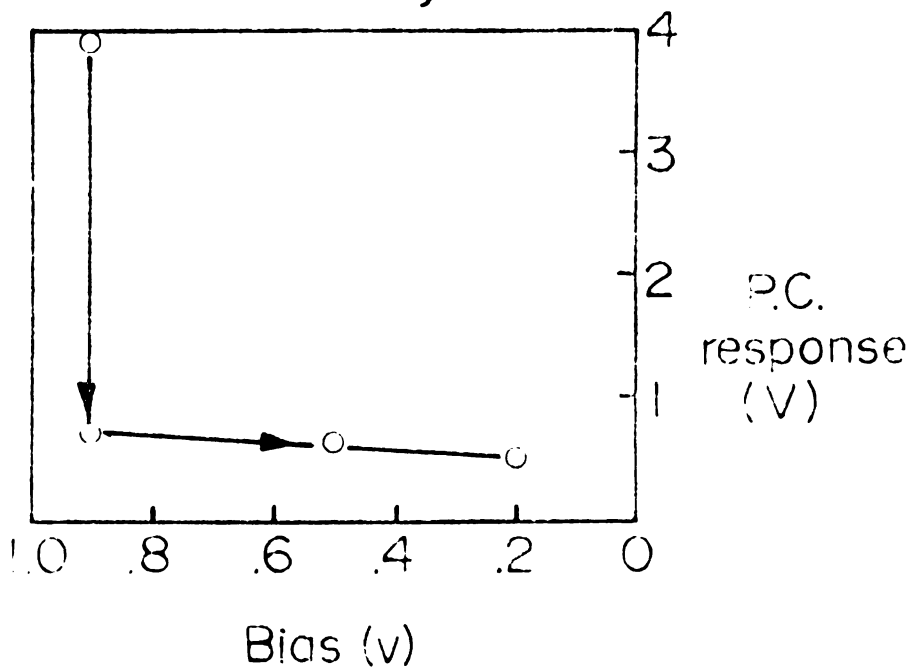
IR filter  
UV filter  
LP47 filter  
LP54 filter

Lockin sensitivity  $500 \mu\text{V}$

93 monolayers



90 monolayers



As the bias potential was moved anodically, the photocurrent response increased. This would be indicative of a higher number of excited dye molecules and faster rate of electron flow from the dye to the semiconductor conduction band. As a result, the supersensitizing agent (oxalate ion) concentration at the dye-solution interface could be rapidly depleted since diffusion of oxalate ion to the interface is not fast enough to maintain a high concentration. Thus, there is a build-up in the  $\text{CuPc}^+$  species concentration which with the bias potential and light probably enhance the desorption and/or decomposition process. Cyclic voltammetry studies indicated a tightly-bound form of CuPc and a more loosely-bound form on the electrode surface. Since a steady photocurrent response was noted after the desorption-decomposition process, it seems the tightly-bound form of dye is retained on the surface. The photocurrent response then appeared to be less potential dependent.

Increasing the oxalate ion concentration appeared to slow down the desorption-decomposition process. Stirring the solution could also retard this process by increasing transport of oxalate ion to the interface. However, the magnetic stirrer frequency coupled with the chopper frequency. This resulted in noise which obscured the photocurrent response.

The actual composition of the retained or tightly-bound layers on the electrodes is not known. Assuming the layers are essentially the same in the electrochemical and photochemical studies, ESCA studies appear to indicate the presence

of an electrochemically active species. It is possible the retained layers are not de-metalled phthalocyanine, but a decomposed form of CuPc; this decomposed form is electrochemically active, i.e. contains double bonds.

#### Covalent Attachment Studies

CuPc was attached to SnO<sub>2</sub> via sulfonamide formation using gamma-aminopropyl-triethoxysilane or N,beta-aminoethyl-gamma-aminopropyl-trimethoxysilane and the sulfonyl chloride form of the dye (Figure 3). The sulfonamide procedure involves loss of HCl and the formation of a nitrogen-sulfur bond. Attachment via a thiol formation using mercaptopropyl-trimethoxysilane and tetraiodated CuPc (Figure 3) was unsuccessful because the dye was insoluble in aqueous media. The reaction should involve loss of HI and the formation of a carbon-sulfur bond between the dye and silane. Since CuPcI<sub>4</sub> was soluble in pyridine, either it or water/pyridine mixtures were also tried without success. The thiol formation has previously worked only in pH 7 buffer with water soluble dyes (58).

#### Spectrophotometric Studies of Covalently-Attached CuPc

An absorption spectrum of CuPc covalently-attached to SnO<sub>2</sub> is shown in Figure 17. Absorption maxima were at 620nm and 694nm corresponding to those of the dye sublimed on SnO<sub>2</sub>. Absorption due to the dye (0.024) indicated approximately  $2.45 \times 10^{13}$  dye molecules present on the surface

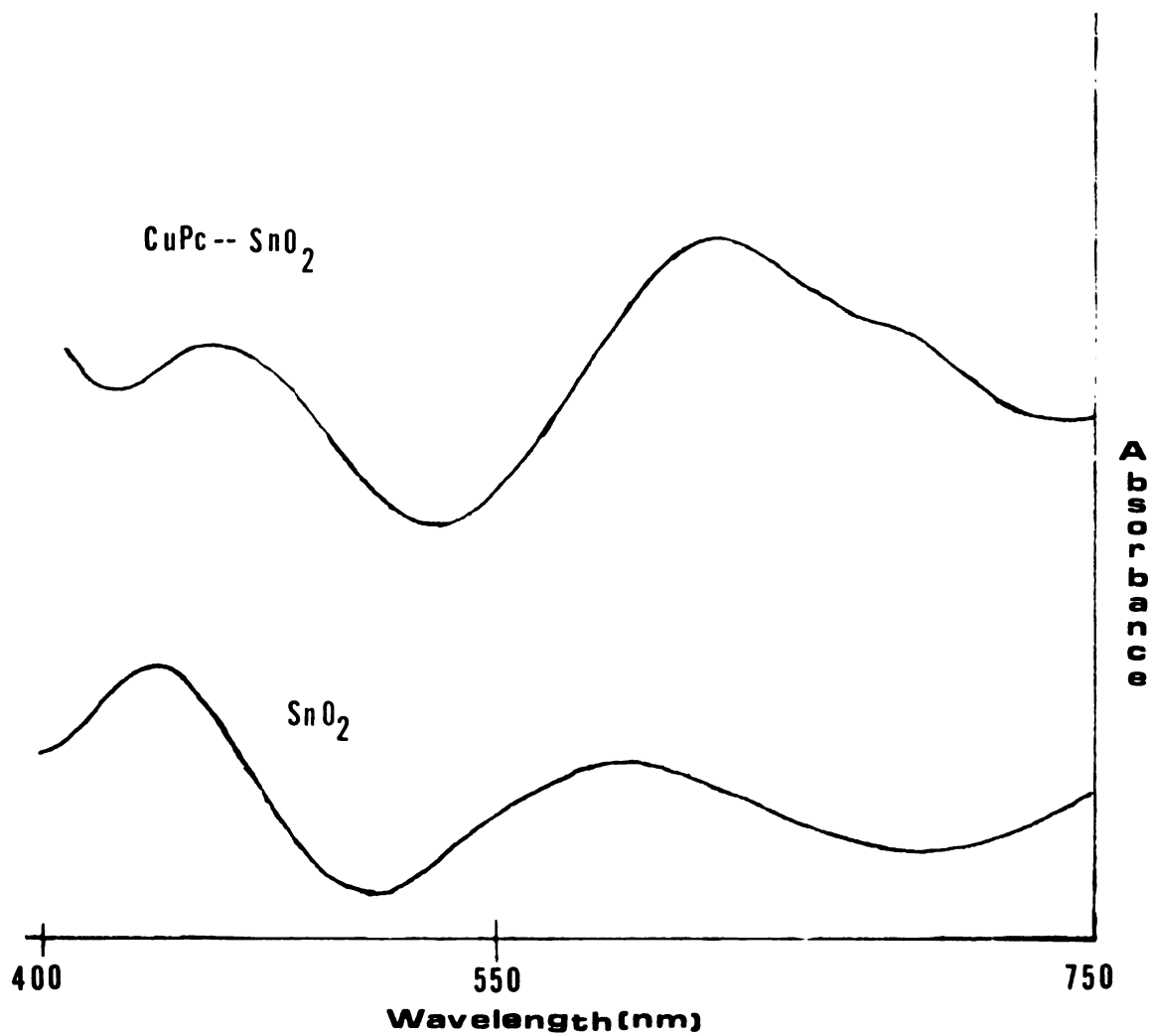


Figure 17. Absorption spectra of clean SnO<sub>2</sub> and covalently-attached CuPc-SnO<sub>2</sub> electrodes.

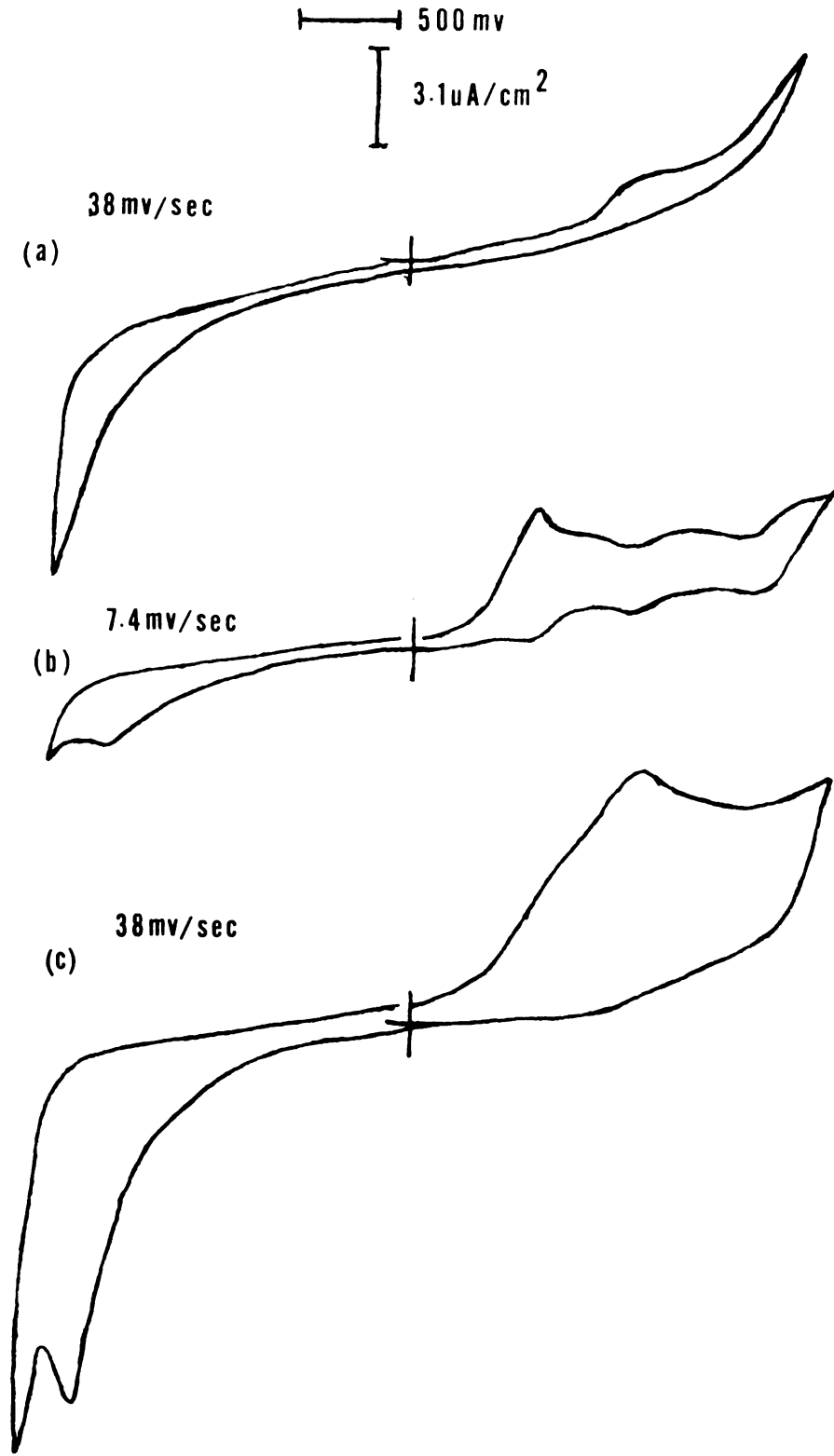
assuming a dye diameter of  $14.3 \text{ \AA}$ , extinction coefficient of  $3.4 \times 10^4 \text{ M}^{-1} \text{ cm}^{-1}$  (27), and a  $0.5 \text{ cm}^2$  sample area. If a  $\text{SnO}_2$  molecule area was  $30 \text{ \AA}^2$  and the dye was arranged perpendicular to the surface, there should be, at most, eight dye molecules for every  $550 \text{ \AA}^2$  of surface, or approximately  $7.35 \times 10^{13}$  molecules/ $0.5 \text{ cm}^2$ . Approximately  $1.03 \times 10^{13}$  molecules/ $0.5 \text{ cm}^2$  would be present if the dye molecules were arranged parallel with the surface. The actual dye arrangement is probably some combination of the above mentioned. The extent of silane coverage, number of active dye attachment sites, and steric hinderance limit the dye coverage.

### Electrochemistry of Covalently-Attached CuPc-SnO<sub>2</sub>

#### Electrodes

The cyclic voltammetry of a chemically-modified electrode in DMSO is shown in Figure 18. Scanning cathodically (cyclic (b)), three reduction waves were observed at -0.55 volts, -1.25 volts, and -1.80 volts vs AgRE. The peaks appeared chemically irreversible with three anodic waves at -0.58 volts, -0.98 volts, and -1.6 volts corresponding to oxidations of the reduction products. An irreversible oxidation of the dye occurred at 1.4 volts vs AgRE. Stirring the electrolyte solution then scanning cathodically again, resulted in cyclic (c); two poorly resolved reductions and an oxidation of the dye were observed. These waves maintained constant magnitude indicating the presence of an electrochemically active species.

Figure 18. Cyclic voltammetry of covalently-attached CuPc-SnO<sub>2</sub> electrode in 0.1 μ TEAP/DMSO.



Cyclic (c) of the covalently-attached dye is quite similar to cyclic (c) of the adsorbed dye (Figure 12). It is conceivable the chemically irreversible waves noted are really the catalytic oxidation and reduction of molecular oxygen since it is well known the phthalocyanines are good catalysts (59). The presence of  $10^{-4}\text{M}$  -  $10^{-6}\text{M}$  oxygen would be enough for the adsorbed or covalently-attached dye to catalyze its electrochemical reduction and oxidation. It is also possible the cyclic corresponds to the oxidation and reduction of a decomposed form of CuPc.

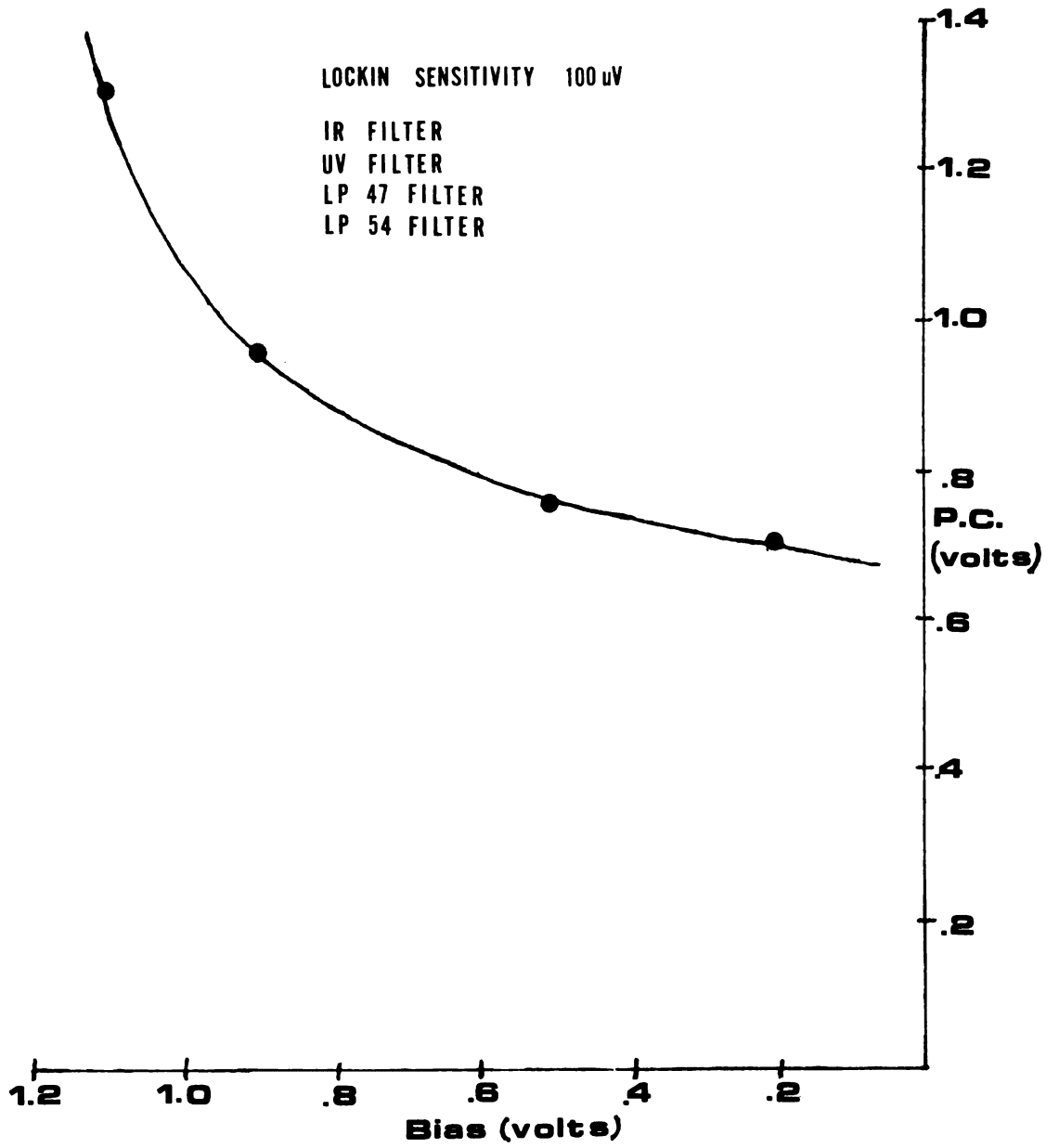
The above spectrophotometric and electrochemical results do not totally confirm the success of the covalent attachment. Therefore, unsilanized  $\text{SnO}_2$  and  $\text{TiO}_2$  were used as controls to insure the results were not those of adsorbed dye. Unsilanized  $\text{SnO}_2$  was allowed to react with the sulfonyl chloride form of the dye. It was then extracted in benzene and water in the manner the derivatized electrodes were. Spectrophotometric studies indicated a clean  $\text{SnO}_2$  surface; cyclic voltammetry of the electrodes also confirmed the absence of any adsorbed dye (Figure 18 (a)).

It is conceivable that the silanized surface of the  $\text{SnO}_2$  could enhance adsorption. However, if the dye was adsorbed, extraction with water would decompose the sulfonyl chloride sites on the CuPc to form tetrasulfonated CuPc which is soluble. Therefore, the dye is most probably covalently-attached to the semiconductor electrode.

Photocurrent Response

The photocurrent response vs anodic bias potential plot of a sulfonamide-linked CuPc-SnO<sub>2</sub> electrode in 0.05M sodium oxalate/pH 7 buffer is shown in Figure 19. The response appears to be potential dependent with its initiation beginning at approximately 0.5 volts vs Ag/AgCl reference electrode. The photocurrent at any given anodic potential was steady over a period of several minutes, and is comparable to the photocurrent response of the adsorbed dye electrode after the desorption/decomposition process is complete. The covalently-attached dye electrode response was approximately one-fourth the final adsorbed dye electrode photocurrent response. Further conclusions concerning the stability and photocurrent response of the covalently-attached dye can not be made without more experimentation.

Figure 19. Photocurrent response vs anodic bias potential of a covalently-attached CuPc-SnO<sub>2</sub> electrode in 0.05M Na<sub>2</sub>C<sub>2</sub>O<sub>4</sub>/pH 7 buffer.



CHAPTER IV  
SUGGESTIONS FOR FUTURE WORK

Future work would consist of several closely related investigations. Better methods of covalent-attachment to increase the phthalocyanine surface coverage would be studied. Efficiency of the photosensitizing process could be increased by using electrodes with several monolayers of covalently-attached dye. This could be accomplished by two methods: (1) coupling of phthalocyanine molecules with cyanuric chloride (60), or (2) coupling of a silicon phthalocyanine derivative with itself (61,62).

Extensive photocurrent studies of the adsorbed and covalently-attached dye electrodes would be carried out. Use of a pulse dye laser would increase the light intensity and photocurrents. Photocurrent response studies using different supersensitizing agents, light aging studies with the chemically-modified electrodes biased at different potentials, and ESCA studies of electrodes in various states of electrochemical and photocurrent treatment would aid in a better understanding of the chemical stability of the dye and kinetics of the photosensitizing process.

**"LIST OF REFERENCES"**

## "LIST OF REFERENCES"

1. M.S. Wrighton, D.S. Gimley, P.T. Wolczonski, A.B. Ellis, D.L. Morse, and A. Linz, Proc. Nat'l Acad. Sci., U.S.A., 72, 1518 (1975).
2. H. Gerischer, Photochemistry and Photobiology, 16, 243 (1977).
3. S. Mishitsuka and K. Tamsru, J. Chem. Soc., London, 73, 705 (1977).
4. T. Osa and M. Fujihira, Nature, 264, 349 (1976).
5. D. Hawn and N.R. Armstrong, unpublished results (manuscript in preparation).
6. T. Osa and T. Kuwana, J. Electroanal. Chem., 22, 389 (1969).
7. V.A. Myamlin and Y.V. Pleskov, "Electrochemistry of Semiconductors," Plenum Press, New York, 1967.
8. S.N. Frank and A.J. Band, J. Amer. Chem. Soc., 97, 7427 (1975).
9. K.G. Allum, R. Hancock, and P. Robinson, J. Organomet. Chem., 87, 293 (1975).
10. G.B. Harper, Anal. Chem., 47, 348 (1975).
11. C.M. Elliott and R.W. Murray, Anal. Chem., 48, 1247 (1976).
12. N.R. Armstrong, A.W.C. Lin, M. Fujihara, and T. Kuwana, Anal. Chem., 48, 741 (1976).
13. P.R. Moser, L. Wier, and R.W. Murray, Anal. Chem., 47, 1882 (1975).
14. P.R. Moser and R.W. Murray, J. Amer. Chem. Soc., in press.

15. B.F. Watkins, J.R. Behling, E. Koriv, and L.L. Miller, J. Amer. Chem. Soc., 97, 3549 (1975).
16. D.G. Davis and R.W. Murray, Anal. Chem., 49, 194 (1977).
17. K. Siegbahn, C. Vordling and A. Fahlmann, et al., "Electron Spectroscopy for Chemical Analysis," Almquist and Wilkells, Uppsala, Sweden, 1967.
18. K. Siegbahn, C. Vordling, K. Hamru, and J. Hedman, et al., "ESCA-Atomic, Molecular and Solid State Structures Studied by Means of Electron Spectroscopy," Almquist and Wilksells, Uppsada, Sweden, 1967.
19. Kane and Larrabee, "Characterization of Solid Surfaces," Plenum Press, New York, 1974.
20. J.T. Yates, Chem. and Eng. News, Aug. 26, (1974).
21. J.T. Yates and T.E. Madey, Surface Sci., 43, 257 (1974).
22. K.S. Kim, T.J. O'Leary, and N. Winograd, Anal. Chem., 45, 2214 (1973).
23. M.J. Dressers and T.E. Madey, Surface Sci., 42. 533 (1974).
24. A.W.C. Lin, N.R. Armstrong, and T. Kuwana, Anal. Chem., in press.
25. J.M. Bolts and M.S. Wrighton, J. Phys. Chem., 80, 2641 (1976).
26. R. Memming, Photochem. and Photobiology, 16, 325 (1972).
27. F.H. Moser and A.L. Thomas, "Phthalocyanine Compounds," ACS Monograph Series, No. 157 (1963).
28. D.H. Busch, J.H. Weber, D.H. Williams and N.J. Rose, J. Amer. Chem. Soc., 86, 5161 (1964).
29. E.A. Lacia and F.D. Verderame, J. Chem. Phys., 48, 2674 (1968).
30. L.D. Rollman and R.T. Iwamot, J. Amer. Chem. Soc., 90, 1455 (1968).
31. A.N. Sidorov, Russian J. Structural Chem., 14, 255 (1973).

32. E.A. Rodyushkuna, B.D. Bereyin, and M.R. Tarasevich, Elektrokhimiya, 9, 410 (1973).
33. Y.M. Stolovitskii, A.Y. Shkuropatov, and V.V. Shichhov, Biofizika, 19, 820 (1974).
34. V.S. Shumov and M. Heyrovsky, J. Electroanal. Chem., 65, 469 (1975).
35. G.A. Alferov and V.I. Sevast'yanov, Elektrokhimiya, 11, 827 (1975).
36. J.P. Randin, Electrochimica Acta., 19, 83 (1974).
37. T.A. Maas, M. Kuijer, and J. Zwart, J. Chem. Soc., Chem. Comm., 86 (1976).
38. Y. Niwa, H. Kobayashi, and T. Tsuchiya, J. Chem. Phys., 60, 799 (1974).
39. M. Zeller and R.G. Hayes, J. Amer. Chem. Soc., 95, 3855 (1973).
40. J.H. Weber and D.H. Busch, Inorg. Chem., 4, 469 (1965).
41. R.W. Higgins and C.L. Hilton, J. Org. Chem., 16, 1275 (1951).
42. Japan Patent No. 19,225.
43. W.F. Kosoncky, S.E. Harrision and R. Stander, J. Chem. Phys., 43, 831 (1965).
44. M. Babai, N. Tshermikooski, and E. Gileadi, J. Electrochem. Soc., 119, 1018 (1972).
45. R.K. Quinn and N.R. Armstrong, J. Vac. Sci. Technol., 12, 160 (1975).
46. D. Sawyer and J. Roberts, "Experimental Electrochemistry For Chemists," John Wiliz and Sons, New York, 1974.
47. Y.S. Shumov, V.I. Sevast'yanov, and G.G. Komissarov, Biofizika, 18, 48 (1973).
48. A. Vogel, "Practical Organic Chemistry," 2nd ed., Wiley, New York, 1966.

49. P.A. Grutsch, M.V. Zeller, and T.P. Fehlner, Inorg. Chem., 12, 1431 (1973).
50. N.R. Armstrong and T.V. Atkison, private communication.
51. K. Bernauer and S. Fallab, Helvetica Chemica Acta, 44, 1287 (1962).
52. D.W. Clac, J.B. Raynor, L.P. Stodulski, and M.R. Symons, J. Chem. Soc. A, 997, (1969).
53. W.P. Gomes and F. Cardon, Z. Phys. Chem., 86, 333 (1973).
54. N.R. Armstrong, private communication.
55. T. Novakov and R. Prins, in "Electron Spectroscopy," Proc. Intern., Conf. Held at Asilomar, Calif. 7-10 Sept. 1971, Ed. D.A. Shirley, Worth-Holland, Amsterdam, 1972.
56. P.A. Larson, J. Elec. Spect. and Related Phenom., 4, 213 (1974).
57. G. Schon, Surface Science, 35, 96 (1973).
58. B.B. Hasenoff, Cand. J. Biochem., 49, 742 (1971).
59. J.R. Goldenstein and A.C.C. Tseung, Nature, 222, 869 (1971).
60. K. Venkatasaman, "The Chemistry of Synthetic Dyes," Academic Press, New York, 1972.
61. Japan Patent 5,711.
62. J.N. Esposito, J.E. Lloyd, and M.E. Kenney, Inorg. Chem., 5, 1979 (1966).
63. R.S. Kirk, Molecular Crystals, 5, 211 (1968).

MICHIGAN STATE UNIVERSITY LIBRARIES



3 1293 03103 8759